7 Pharmacokinetic Modeling Program (PKMP): A Software for PK/PD Data Analysis

Ajit K. Shah

Contents

A. K. Shah (✉)
APL, Eden Prairie, MN, USA
e-mail: shah.ajit@aplanalytics.com

J. K. Patel, Y. V. Pathak (eds.), *Pharmacokinetics and Pharmacodynamics of Nanoparticulate Drug Delivery Systems*, https://doi.org/10.1007/978-3-030-83395-4_7

Abstract

In drug research and development, pharmacokinetics, which characterizes absorption, distribution, metabolism, and elimination of the drug from the body after its administration in animals and humans, plays an important role in delineating the dose-response relationship, either for toxicity in animal studies or safety and efficacy analysis in human clinical trials. The following is an overview of the pharmacokinetic modeling program (PKMP) developed to perform data analysis to support drug research and development. PKMP is a web-based commercial program created using the open source codes for Java coding language and R libraries. The web-based platform allows easy and secure access to the program using any Internet browser, and the program is independent of operating systems, such as MacOS or Windows. The program has been extensively tested for validation and verification of every module for its quality and functionality. Pharmacokinetic, pharmacodynamic, statistical analysis, dissolution, IVIVC, simulation, modeling, and reporting are some of its main functionalities, allowing for a wide range of data analyses to support drug product evaluation and development during different phases of drug development.

Keywords

Pharmacokinetics · Pharmacodynamics · Dissolution · IVIVC · Modeling · Simulation · Toxicokinetics · Interspecies scaling · Biopharmaceutics · Bioequivalence

1 Introduction

The drug development process involves discovery phase, preclinical research, clinical research, and regulatory approval for marketing. From start to finish, the drug development takes 10–15 years, and the average research and development cost is estimated to be $2.6 billion [1]. In each phase of drug research and development, pharmacokinetics, which characterizes absorption, distribution, metabolism, and elimination of the drug from the body after its administration in animals and humans, plays an important role in delineating the dose-response relationship, either for toxicity in animal studies or safety and efficacy analysis in human clinical trials. Therefore, pharmacokinetic data analysis has become an essential part in the following key areas of drug development, including, but not limited to, lead identification/optimization, dose-response analysis, bioequivalence analysis of drug products, in vitro–in vivo correlations for formulations, dissolution data analysis, modeling, and simulations. These analyses are critical in drug development for cost and time savings. The generic drug products are created to provide medicines at a reduced cost and involve drug development based on demonstrating pharmacokinetic equivalence of systemic drug concentrations of generic and innovator products. The pharmacokinetic data analysis nowadays is performed using commercial software packages having a wide range of capabilities for data analysis, visual display, and simulations. The following is an overview of the pharmacokinetic modeling program (PKMP) developed to perform these types of data analysis

to support drug research and development. Theoretical aspects of each analysis and functionalities of PKMP are extensively published elsewhere [2–4]. The computational algorithms in PKMP are based on the pharmacokinetic and statistical theories from textbooks [2–4], published literature [5], and regulatory guidance documents from the Food and Drug Administration (FDA) of the United States.

2 Organization of PKMP

The organization of PKMP data analysis modules, file upload functionalities, sample files for data analysis, and the last file analyzed are displayed on the dashboard of program as shown in Fig. 7.1. The user is required to have a user ID and password to access the dashboard and analysis modules. The typical file format for upload is Excel data types, such as XLS, XLSX, or CSV. Once the file is selected for upload, its association for the type of analysis is required using the radio buttons provided on the dashboard. Sample data files for different types of analysis are provided to get used to the data format needed for an analysis module. Previously performed analyses and their reports are stored and can easily be accessed from the dashboard.

3 Analysis Modules

The data analysis modules are displayed on the left side of the dashboard. Each module has submodules for appropriate data analysis and is described below.

3.1 NCA-PK

Noncompartmental methods (NCA-PK) for pharmacokinetic parameters are based on estimation of the area under a curve of drug concentration vs. time data following the drug administration by either extravascular (oral, intramuscular, topical, etc.) or vascular routes (intravenous, intra-arterial, etc.). Noncompartmental methods do not require the assumption of specific compartmental model for either drug or metabolite. The methods assume input, elimination, and sampling from the central compartment [2, 3, 5].

3.2 Extravascular/IV Bolus/IV Infusion

The plasma concentration time profiles following oral administration of a drug are shown in Fig. 7.2.

To compute noncompartmental pharmacokinetic parameters for a plasma concentration vs. time profile, as shown in Fig. 7.3, the curve is divided into a number of trapezoids by drawing a vertical line for each concentration corresponding with time point on x-axis.

The following methods [2] are used to compute area under each trapezoid:

Linear Trapezoidal Rule

$$\mathrm{AUC} = \sum_{i=n}^{i=0} \frac{C_i + C_{i+1}}{2} \cdot \ t \qquad (7.1)$$

C_i and C_{i+1} are the plasma concentrations at time t_i and t_{i+1}, respectively, and Δt is the sampling time interval. After a single oral dose of a drug, C_i at time 0 is typically zero. C_i at time 0 has a positive value following a single intravenous bolus dose of drug. Therefore, the concentration at time 0 can be extrapolated back using either linear back extrapolation, a user-defined value, or a compartmental back extrapolation for one, two, or three compartment body models for an IV dose. The area under the curve is summation of individual area under each trapezoid up to last time of sampling t.

Log-Linear Trapezoidal Rule

In cases where concentrations are more curved between the sampling time points, area estimates are obtained using the log-linear trapezoidal rule:

$$\mathrm{AUC} = \sum_{i=n}^{i=1} \frac{\left(C_i - C_{i+1}\right)}{\left(\ln C_i - \ln C_{i+1}\right)} \bullet \ t \qquad (7.2)$$

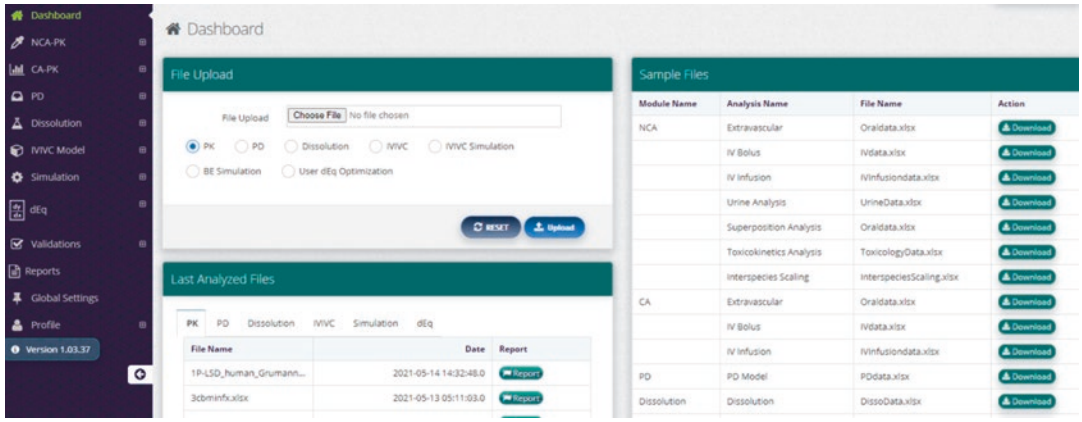

Fig. 7.1 The organization of PKMP

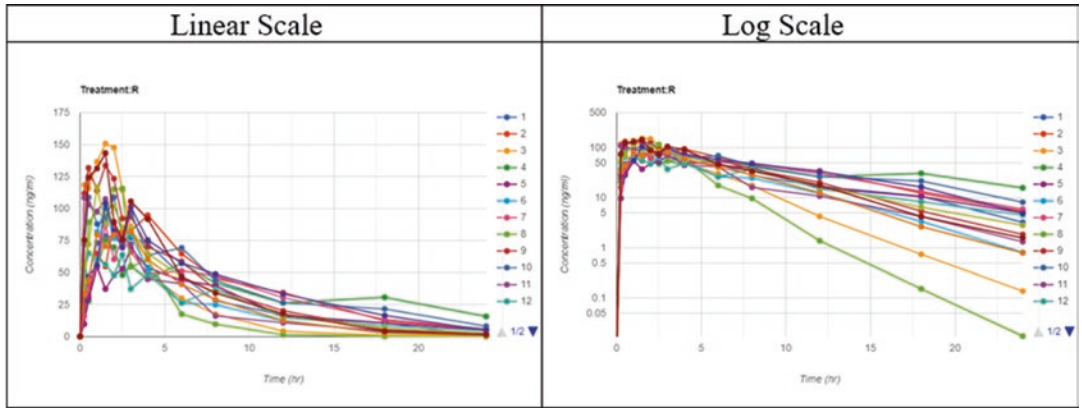

Fig. 7.2 Plasma concentration vs. time profiles in subjects following oral administration of a single dose of a drug

3.3 Mixed Log-Linear

This method is a combination of above linear and log-linear trapezoidal methods applied to up and down parts of a concentration time profile.

Maximum drug concentration (C_{max}) and time to C_{max} (T_{max}) are estimated based on observed data as shown in Fig. 7.3. The terminal phase elimination rate constant, Kel, is estimated from the slope of the concentration-time data during the log-linear terminal phase using least squares regression analysis. For the Kel calculation, PKMP uses the last four data points by default (Fig. 7.4). The calculated regression parameters (slope and intercept), their statistics for R^2 and R^2-adjusted, and number of data points used are displayed. The user can modify this, as appropriate, by clicking and selecting other data points. The updated calculations are saved and retained by the program.

The terminal phase elimination half-life ($T_{1/2}$) is calculated as

$$T_{1/2} = \frac{0.693}{\text{Kel}} \tag{7.3}$$

The area under the concentration-time curve (AUC_{0-t}) from time 0 to the last measurable concentration (C_t) at time t is calculated using the trapezoidal method and extrapolated to $AUC_{0-\infty}$ using

$$\text{AUC}_{(0-\infty)} = \text{AUC}_{(0-t)} + \frac{C_t}{\text{Kel}} \tag{7.4}$$

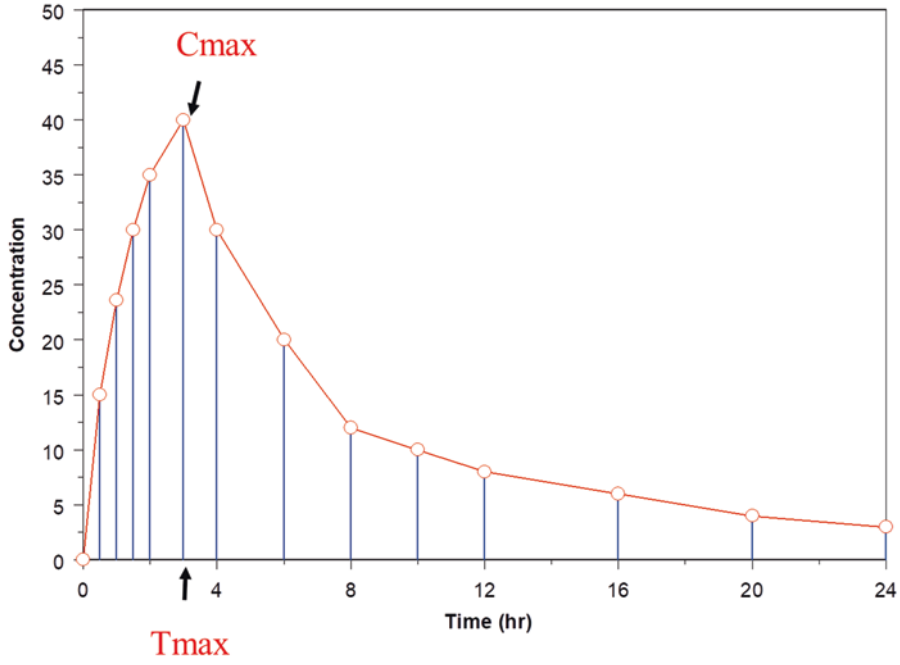

Fig. 7.3 Representation of plasma concentration vs. time profile divided into trapezoids for the noncompartmental method calculations

Partial areas under the curve also can be computed as per the selection of time points such as 0–2 hours, 4–8 hours, etc., and analysis can be repeated for all subjects.

The apparent total body clearance for oral administration is calculated as

$$\mathrm{CL}/F = \frac{D_{\mathrm{oral}}}{\mathrm{AUC}_{(0-\infty)}} \tag{7.5}$$

For an intravenous dose, the term F for bioavailability is considered 1.

The apparent volume of distribution during the terminal phase after oral administration is calculated as

$$V_{\mathrm{d}}/F = \frac{\mathrm{CL}_{\mathrm{oral}}}{\mathrm{Kel}} \tag{7.6}$$

The apparent volume of distribution at steady state (V_{ss}) or equilibrium after intravenous administration is calculated as

$$V_{\mathrm{ss}} = \mathrm{CL}\cdot\mathrm{MRT} \tag{7.7}$$

where

MRT is the mean residence time and is calculated as

$$\mathrm{MRT} = \frac{\int_0^\infty t.Cdt}{\int_0^\infty Cdt} = \frac{\mathrm{AUMC}}{\mathrm{AUC}} \tag{7.8}$$

For infusion administration, the duration of infusion is included in computation.

AUMC is area under the moment curve calculated by means of trapezoidal rule and extrapolated to infinity using the following equations:

$$\mathrm{AUMC} = \sum_{i=n}^{i=0} \frac{t_i.C_i + t_{i+1}.C_{i+1}}{2} \bullet\ t \tag{7.9}$$

and

$$\mathrm{AUMC}_{(0-\infty)} = \mathrm{AUMC} + \frac{t_{\mathrm{last}}.C_{\mathrm{last}}}{\mathrm{Kel}} + \frac{C_{\mathrm{last}}}{\mathrm{Kel}^2} \tag{7.10}$$

The computation of NCA PK parameters is shown in Table 7.1:

The following statistical analysis can be performed after completion of NCA [6].

Kel	Slope	Intercept	R^2	R^2_Adj	No. of Points
0.1295	−0.1295	83.9906	0.9590	0.9385	4

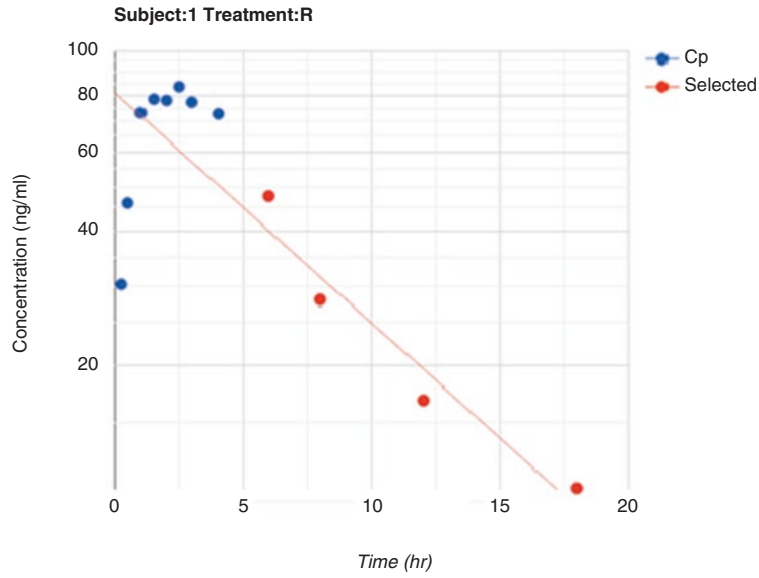

Fig. 7.4 Calculation of Kel using concentration-time data during the log-linear terminal elimination phase. Default last four points are used in the calculation which can be changed as appropriate by selecting other data points

4 Bioequivalency (BE) Analysis (Two-Way Crossover Study)

Bioequivalency for two orally administered drug products is required to demonstrate the same rate and extent of absorption between the active drug ingredient or moiety in the test (*T*) product and the reference (*R*) drug product to ensure therapeutic equivalence. Bioequivalency assessment between formulations is needed during different clinical stages of drug development. Additionally, it is required for the generic product abbreviated new drug application submission. The study is conducted as a two-formulation, two-period, and two-sequence crossover design in a group of subjects administered test and reference treatments. Blood samples are obtained after administration of products to quantitate drug or metabolite concentrations and pharmacokinetic parameters [6].

For the average bioequivalence calculations, AUC and C_{max} of *T* and *R* products are log transformed. A 90% confidence interval for the *T* to *R* parameter ratio of the averages (population geometric means) is computed using an analysis of variance (ANOVA) model including sequence, period, and treatment as fixed effects and subject within the sequence as random effect. To establish BE, the calculated confidence interval should fall within a BE limit, usually 80–125% for the *T* to *R* ratio of the parameter averages (Table 7.2).

5 Repeated BE Analysis

Repeated bioequivalence studies in which test (*T*) and reference (*R*) treatments are administered repeatedly over three or four periods. The analysis is performed as per the FDA guidance [6], using a restricted or residual maximum likelihood (REML) procedure.

The following is a model for the replicated BE studies as described in the FDA guidance document [6] that assumes a four-period design with equal replication of *T* and *R* in each of sequences, with an assumption of no (or equal) carryover effects (equal carryovers go into the period effects):

$$Y_{ijkl} = \mu_k + \gamma_{ikl} + \delta_{ijk} + \varepsilon_{ijkl} \qquad (7.11)$$

where

$i = 1,\ldots.s$ indicates sequence

Table 7.1 Computation of noncompartmental analysis pharmacokinetic parameters

Subject	Treatment	Period	Sequence	Dose	Kel	R^2	$T_{1/2}$	T_{max}	C_{max}	Time Reg Start	Time Reg End	T_{lag}	C_{last}/C_{max}	AUC_{0-t}	AUC_{All}	AUC_{0-inf}	$AUC_{0-t/0-inf}$	$AUMC_{0-t}$	$AUMC_{0-inf}$	MRT_{0-t}	MRT_{0-inf}	V_d/F	Cl/F
Units				mg	1/hr		hr	hr	ng/ml	hr	hr	hr		ng/ml*hr	ng/ml*hr	ng/ml*hr		ng/ml*hr^2	ng/ml*hr^2	hr	hr	L	L/hr
1	R	1	RT	100	0.12	0.94	5.88	2.5	83.72	6	18	0	0.13	644.16	676.34	735.21	0.88	3731.24	6142.84	5.79	8.36	1154.4	136.0
2	R	2	TR	100	0.14	0.99	4.99	4	94.75	8	24	0	0.06	889.12	889.12	927.93	0.96	6664	7875.09	7.5	8.49	776.2	107.8
3	R	1	RT	100	0.30	1.00	2.31	1.5	150.86	8	24	0	0	625.14	625.14	625.6	1	2115.29	2127.8	3.38	3.4	532.2	159.8

Table 7.2 Bioequivalence analysis for a two-way crossover study

Parameter name: $AUC_{(0-t)}$						
Source	*df*	SS type I	SS type III	MSE	*F*-value	Pr >/*i*
Sequence	1	0.002	0.002	0.002	0.014	0.9068
Subj(Sequence)	10	1.594	1.594	0.159	29.431	4.32E-06
Period	1	0.021	0.021	0.021	3.784	0.0804
Trt	1	0.000397	0.000397	0.000	0.073	0.7921
Model	13		1.618	0.124	22.969	
Error	10		0.054	0.005		
			90% confidence interval			
Trt difference log scale			Lower		Upper	
0.00813			−0.0463		0.0626	
Original scale%			*T/R* ratio lower%		*T/R* ratio upper%	
100.82			95.47		106.46	

Similar analysis for C_{max} or other parameters can be performed

$j = 1, \ldots n$ indicates subject within sequence i

$k = R, T$ indicates treatment

$l = 1, 2$ indicates replicate on treatment k for subjects within sequence i

Y_{ijkl} = the response of replicate l on treatment k for subject j in sequence i

γ_{ikl} = the fixed effect of replicate l on treatment k in sequence i

δ_{ijk} = the random subject effect for subject j in sequence i on treatment k

ε_{ijkl} = the random error for subject j within sequence i on replicate l of treatment k

The ε_{ijkl}'s are assumed to be mutually independent and identically distributed as

$$\varepsilon_{ijkl} \sim N\left(0, \sigma \mathrm{Wk}^2\right)$$

for $i = 1 \ldots s$, $j = 1 \ldots n$, $k = R, T$, and $l = 1, 2$.

In addition, the random subject effects are assumed to be mutually independent.

An example of four-period crossover study design is shown in Table 7.3.

The BE analysis for the four-period crossover repeated study for log transformed AUC for *T* and *R* treatments is displayed in Table 7.4. Similar analysis for the C_{max} can also be computed. Additional statistical results for summary, ANOVA, LSMEAN, LSMDIFF, confidence intervals, correlation coefficients, residuals, and ratio test are also computed.

6 Analysis of Variance (ANOVA)

ANOVA models for parallel or repeated groups with equal or unequal sample sizes (using Welch's correction) for comparison between the means can be performed. An example of ANOVA for parallel groups is shown in Table 7.5.

7 Dose Proportionality Analysis

Dose proportionality between the pharmacokinetic exposure parameters, such as C_{max} and AUC, and administered dose is assessed to evaluate the linearity in the pharmacokinetic of a drug. This ensures predictability in increase in drug exposure as measured by C_{max} and AUC, meaning twofold increase in dose results in a proportional twofold increase in exposure. Dose proportionality is evaluated by the following analysis:

7.1 Linear Model

$$y = m \cdot x + b \qquad (7.12)$$

where

y = PK parameter

m = slope

Table 7.3 Example of a four-period repeated crossover plasma concentration data

Subject	Time (hr)	Dose(mg)	Sequence	Treatment	Period	*Cp* (ng/mL)
1	0.00	100	RRTT	R	1	0.00
1	0.25		RRTT	R	1	30.36
1	1.00		RRTT	R	1	73.08
1	0.00	100	RRTT	R	2	0.00
1	0.25		RRTT	R	2	41.93
1	1.00		RRTT	R	2	132.30
1	0.00	100	RRTT	T	3	0.00
1	0.25		RRTT	T	3	30.36
1	1.00		RRTT	T	3	73.08
1	0.00	100	RRTT	T	4	0.00
1	0.25		RRTT	T	4	41.93
1	1.00		RRTT	T	4	132.30

Data for additional time points and subjects

x = dose
b = intercept

An example of dose proportionality for a PK parameter, $AUC_{(0-t)}$, is shown in Fig. 7.5.
where

y = PK parameter
b = coefficient
m = exponent
x = dose

An example of dose proportionality using the power model for a PK parameter, $AUC_{(0-t)}$, is shown in Fig. 7.6.

7.3 Dose Normalization

Pharmacokinetic parameter is normalized to the lowest dose as shown in Table 7.6 and analyzed to assess dose proportionality.

Normalized C_{max} is obtained as C_{max}/dose/lowest dose (Fig. 7.7).

8 Urine Data Analysis

Urinary excretion is important in understanding the routes of elimination of a drug from the body to account for the mass balance. Urinary excretion rate [2] involves measurement of drug concentration in the urine over the urine collection interval and is calculated as

7.2 Power Model

$$y = b \cdot x^m \tag{7.13}$$

$$\log y = \log b + m \log x \tag{7.14}$$

$$\frac{dXu}{dt} = \frac{Cu \cdot Vu}{t} \tag{7.15}$$

where

dXu/dt = urinary excretion rate
Vu = urine volume
Δt = urine collection interval

The renal clearance of a drug is calculated as

$$CL_r = \frac{Xu}{AUC} \tag{7.16}$$

where

CL_r = renal clearance
Xu = amount of drug in urine over the interval t
AUC = area under the plasma concentration-time curve over time t

The computation of urinary data from the PKMP analysis is shown in Table 7.7, and graphical output for a selected plot is shown in Fig. 7.8.

Table 7.4 Bioequivalence analysis of AUC for the four-period crossover repeated study for test (*T*) and reference (*R*) treatments

Treatment	LS means estimate	Standard error	DF	*T*-value	Lower CI	Upper CI	
T	6.64	0.047	22.9	141.258	6.55	6.74	
R	6.64	0.047	22.9	141.258	6.55	6.74	
LS means difference				90% CI		95% CI	
Treatment	Estimate	Standard error	DF	Lower	Upper	Lower	Upper
T–R	0.0	0.0509	44	−0.0855	0.0855	−0.1026	0.1026
Original scale ratio (%)				90% CI		95% CI	
Estimate				Lower	Upper	Lower	Upper
100.0				91.8	108.9	90.3	110.8

Table 7.5 Analysis of variance of $AUC_{(0-t)}$ comparison for a parallel group study

ANOVA					
Effect source	Sum of squares	Degree of freedom	Mean square	*F*-value	Prob > *F*
Treatment	0.308	1	0.308	6.857	0.014
Error	1.346	30	0.045		
Total	1.653	31			

Confidence interval						
Source	Group 1 vs. Group 2					
Difference	Standard error	Degree of freedom	*T*-value	CI.low	CI.high	*P*-value
−0.196	0.075	30	1.697	−0.323	−0.069	0.014

Group comparison						90% CI		
Group	*N*	Geo. mean	%CV	Ratio	Point est.(%)	Low	High	*P*-value
Group 1	16	694.71	21.97	GP1/GP2	82.19	72.38	93.33	0.01
Group 2	16	845.21	19.97					

Similar analysis for C_{max} and other PK parameters can be performed

9 Superposition Analysis

The principle of superposition [2] allows for the prediction of concentration-time curve after multiple consecutive doses based on the drug concentration-time data obtained after a single dose. The basic assumptions are that the drug is eliminated by first-order pharmacokinetics and the pharmacokinetics of the drug is linear. Based on the calculations of terminal elimination rate constant, dose, and intervals (equal or unequal) and number of doses, superposition analysis for data in Table 7.8 is performed as shown in Fig. 7.9.

10 Toxicokinetics

In toxicokinetic studies, mainly in mice, rats, and other rodents, the generation of a complete concentration-time profile for each animal is difficult due to the limited blood volume that can be drawn. In such a scenario, a single blood sample is obtained from each animal, and several animals are used to generate the complete concentration-time profile over a sampling time period. As the animals are sacrificed after the sampling, this is also called "destructive sampling" method [7]. An example of such a data is shown in Table 7.9.

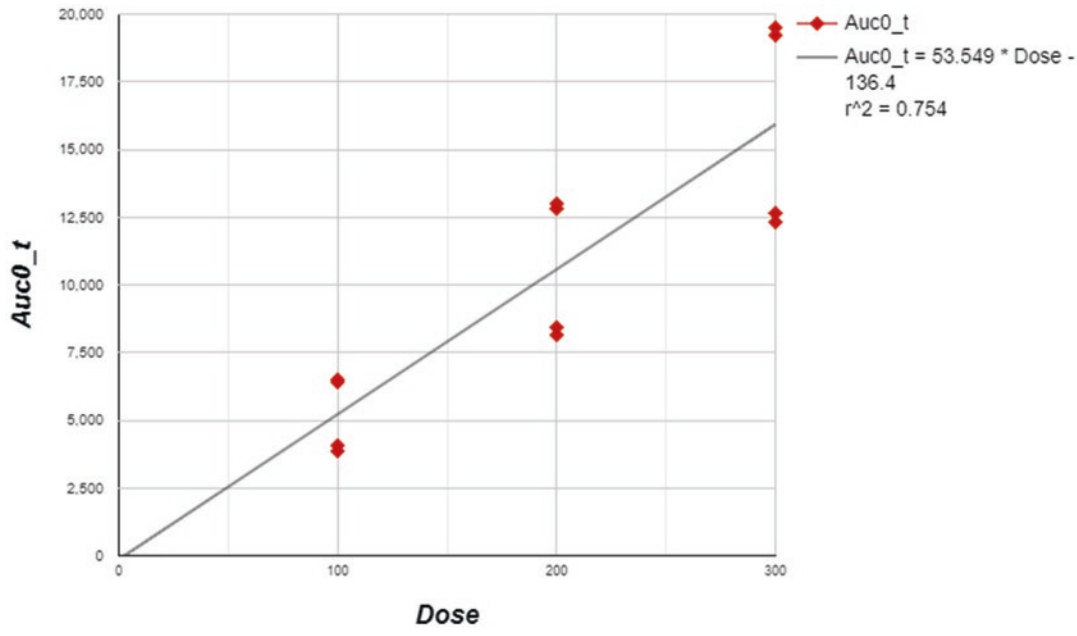

Fig. 7.5 Dose proportionality analysis using the linear model for $AUC_{(0\text{-}t)}$

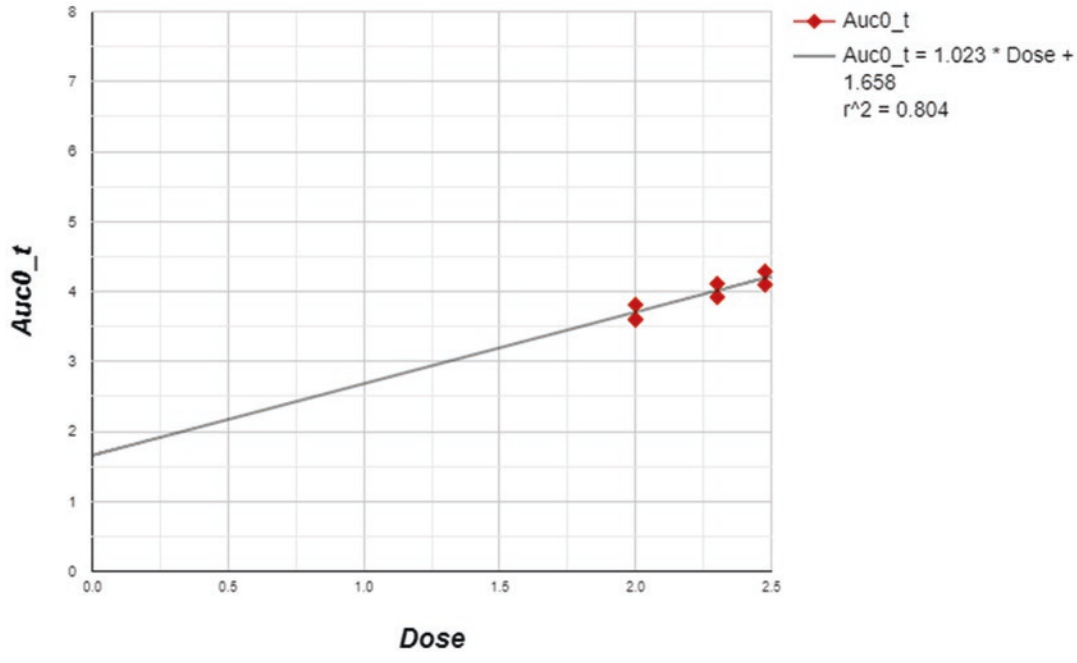

Fig. 7.6 Dose proportionality analysis using the power model for $AUC_{(0\text{-}t)}$

Table 7.6 Dose normalization of a PK parameter

Dose (mg)	C_{max} (mcg/ml)	Normalized C_{max}
100	449	449
100	292	292
100	871	871
100	348	348
200	898	449
200	584	292
200	1742	871
200	696	348
300	1347	449
300	876	292
300	2613	871

Normalized C_{max} is obtained as C_{max}/Dose/lowest dose

11 Interspecies Scaling

Interspecies scaling in pharmacokinetics allows for the prediction of in vivo drug disposition behavior in humans from the experimental observations made in one or more species. Interspecies scaling of the pharmacokinetic processes of absorption, distribution, and clearance of drugs can be performed by allometry [9, 10]. The allometric approach involves estimation of the pharmacokinetic parameters – clearance, half-life, volume of distribution, etc. – in humans based on their relationship to body mass in several test animal species. PKMP interspecies scaling module includes the following methods for prediction of human pharmacokinetics and estimation of a maximum safe starting dose (MSSD) in initial clinical trials for drugs in human subjects as per FDA guidance [11].

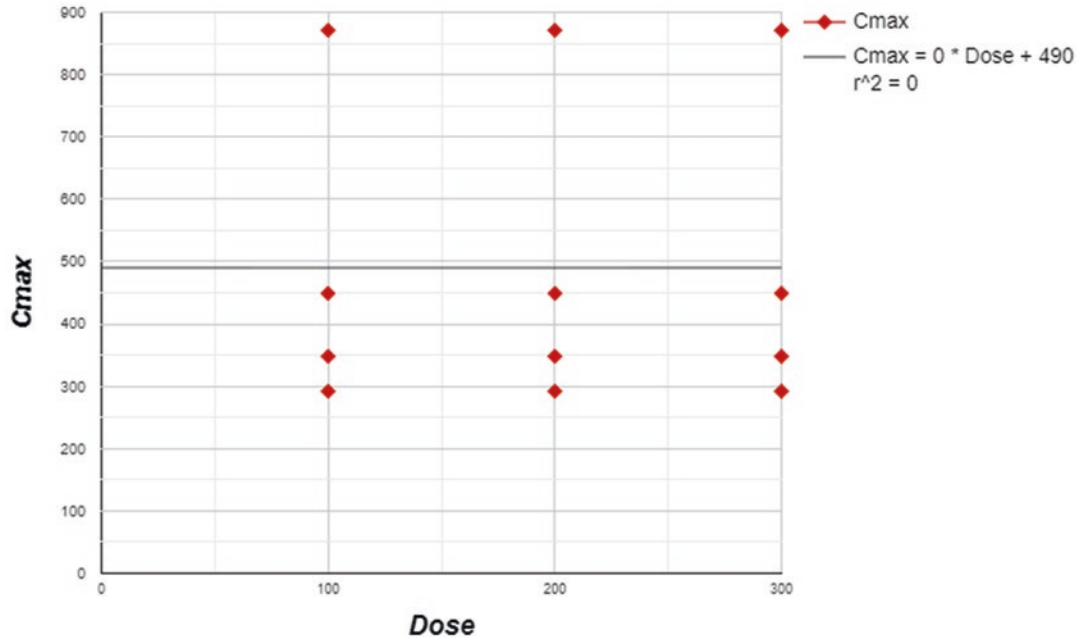

Fig. 7.7 Dose proportionality of C_{max} using the dose normalization method

The analysis of this type of toxicokinetic data can be performed as follows using the toxicokinetic module of PKMP as shown in Table 7.10.

An ANOVA can be performed to determine the differences in the treatments administered as well as the bootstrap analysis [8] to simulate the data.

Table 7.7 Urine concentration data analysis

Subject	Treatment	Time (hr)	Concentration (mg/ml)	Volume (ml)	Dt (hr)	Tm (hr)	Xu_Int (mg)	CUM_Xu (mg)	Dxu_Dt (mg/hr)	Xu_Inf_Xu (mg)	%Dose	AUC (mg/ml*hr)	CL_R (ml/hr)
1	A	0	0	1	0	0	0	0	0	59.58	0	50	0.02
1	A	1	4.02	1	1	0.5	4.02	4.02	4.02	55.56	6.7	50	0.02
1	A	2	3.75	1	1	1.5	3.75	7.77	3.75	51.81	12.95	50	0.02
1	A	3	3.49	1	1	2.5	3.49	11.26	3.49	48.32	18.77	50	0.02
1	A	6	9.15	1	3	4.5	9.15	20.41	3.05	39.17	34.02	50	0.02
1	A	12	13.47	1	6	9	13.47	33.88	2.25	25.7	56.47	50	0.02
1	A	24	14.75	1	12	18	14.75	48.63	1.23	10.95	81.05	50	0.02
1	A	36	6.42	1	12	30	6.42	55.05	0.54	4.53	91.75	50	0.02
1	A	48	2.79	1	12	42	2.79	57.84	0.23	1.74	96.4	50	0.02
1	A	60	1.22	1	12	54	1.22	59.06	0.1	0.52	98.43	50	0.02
1	A	72	0.52	1	12	66	0.52	59.58	0.04	0	99.3	50	0.02

Dt collection interval, *Tm* midpoint of collection interval, *Xu_Int* amount excreted over a collection interval, *CUM_Xu* cumulative amount excreted, *Dxu_Dt* excretion rate, *Xu_inf_Xu* amount at infinity-Xu_int, CL_R renal clearance

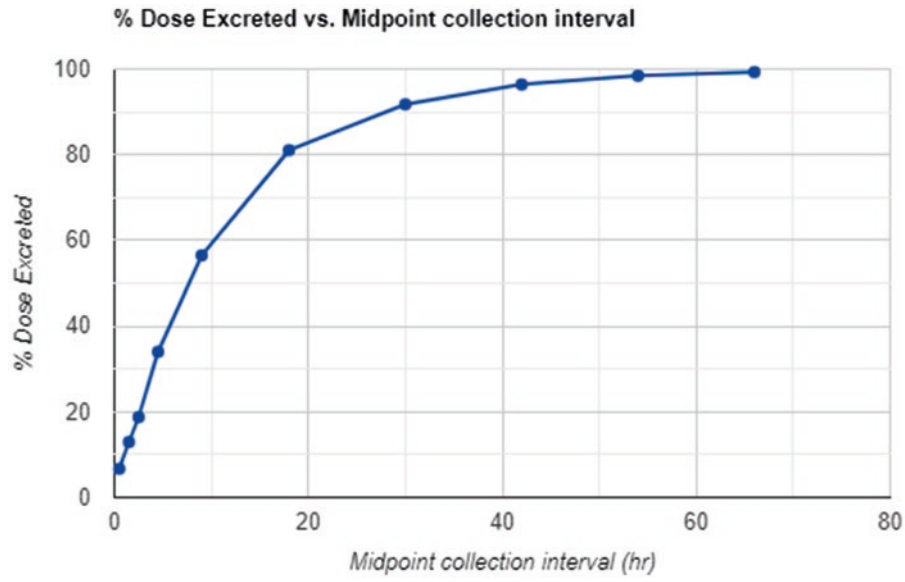

Fig. 7.8 Urinary excretion plot for the % dose excreted and the midpoint of urine collection interval for a drug

Table 7.8 Example of a plasma concentration-time data for a subject for the superposition analysis

Subject	Time (hr)	Concentration (ng/mL)	Dose (mg)
1	0	0	100
1	1	255	
1	2	447	
1	3	449	
1	4	410	
1	6	226	

12 Method 1: NCA

In order to perform analysis using this method, pharmacokinetic data after an intravenous administration of a drug in three or more animal species, such as mice, rats, and dogs, are needed. Intravenous data is preferred for the complete bioavailability of a drug, although extravascular route PK data can be used with consideration to differences in bioavailability across the species. In this method, the pharmacokinetic parameters, CL and V_d, among animal species are correlated as exponential functions of body weight or body surface area (BSA) using the simple allometric equation below, as shown in Fig. 7.10:

$$Y = a \cdot W^b \tag{7.17}$$

or its logarithmic transformation.

$$\log Y = \log a + b \log W \tag{7.18}$$

where

Y = pharmacokinetic parameter
W = body weight
a = allometric coefficient
b = allometric exponent

Similar analysis is done for a V_d parameter for human prediction as shown in Table 7.11.

13 Method 2: PK Parameters

In this method, PK parameters from animal species are converted to human parameters or animal parameters using the BSA ratio extrapolation. For example, human and mouse BSA are 1.8 and 0.007 m^2, respectively, and the human-to-mouse BSA ratio is 257. For a mouse CL value of 5 mL/hr, the human CL can be predicted as product of

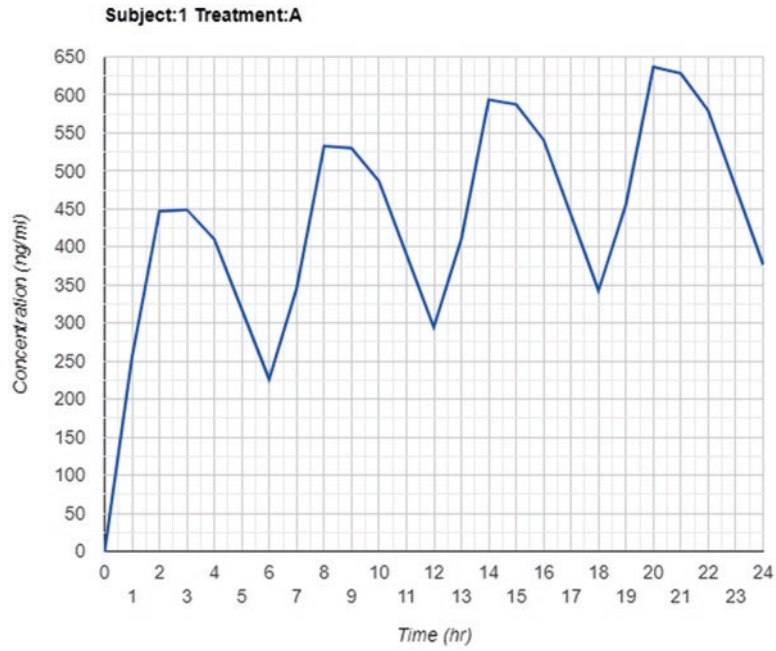

Fig. 7.9 Superposition analysis of a data in Table 7.8 based on Kel, 0.057 (/hr); dosing interval (τ), 6.0 hour; and number of steps, 4

Table 7.9 Example of a toxicokinetic data collected in a limited sampling method with each animal providing one blood sample

Mouse#	Treatment	Dose (mg/kg)	Time (hr)	*Cp* (mcg/mL)
1	A	50	0	0.66
6	A		0	0.32
11	A		0	0.34
16	A		0	0.44
2	A		1.5	0.059
7	A		1.5	0.031
12	A		1.5	0.084
17	A		1.5	0.082
…	…	…	…	…

257 and 5 equal to 1285 mL/hr. A similar approach can be used for prediction of V_d.

14 Method 3: Human Equivalent Dose (HED) (Table 7.12)

HED from an animal's no observed adverse effect level (NOAEL) is calculated as per the FDA guidance [11] using

$$\text{HED} = \text{animal NOAEL} / \text{HED factor} \tag{7.18}$$

or

$$\text{HED} = \text{animal NOAEL} \times \left(\text{Wanimal} / \text{Whuman}\right)^{(1-b)} \tag{7.19}$$

where

W = body weight
b = allometric exponent (typically = 0.67)

15 Dose Escalation

The phase 1 clinical trials are conducted in a dose escalation manner to determine an optimal recommended dose or maximum tolerated dose for a new compound for further testing in phase 2 trials. The dose escalation scheme in phase 1 trials is based on the careful evaluation of safety consideration both to study subjects and to attain the goals of trial [12]. Typically, the starting dose for the phase 1 clinical studies is selected using NOAEL from animals and escalated using either empiric, modified Fibonacci, or logarithmic increments. The PKMP computes and provides these dose escalation schemes as shown in Table 7.13, and these dose escalation schemes

Table 7.10 Toxicokinetic analysis of a limited sampling data

Treatment	Dose	Kel	R^2	$T_{1/2}$	T_{max}	C_{max}	T_{lag}	C_{last}/C_{max}	AUC_{0-t}	AUC_{All}	AUC_{0-inf}	$AUC_{0-t/0-inf}$	$AUMC_{0-t}$	$AUMC_{0-inf}$	MRT_{0-t}	MRT_{0-inf}	V_d/F	Cl/F	AUC_{VAR}	AUC_{SEM}
Units	mg/kg	1/hr		hr	hr	mcg/ml	hr		mcg/ml*hr	mcg/ml*hr	mcg/ml*hr		mcg/ml*hr^2	mcg/ml*hr^2	hr	hr	L/kg	L/hr/kg		
A	50	0.747	0.943	0.927	0	0.043	0	0.021	0.047	0.049	0.048	0.974	0.031	0.039	0.67	0.814	1368	1022	2.48	0.007
B	150	0.646	0.812	1.072	0	0.272	0	0.047	0.342	0.361	0.362	0.944	0.28	0.412	0.819	1.137	640	414	0.011	0.047
C	600	0.975	0.996	0.71	0	0.464	0	0.007	0.563	0.568	0.566	0.993	0.415	0.435	0.737	0.768	1085	1059	0.032	0.08

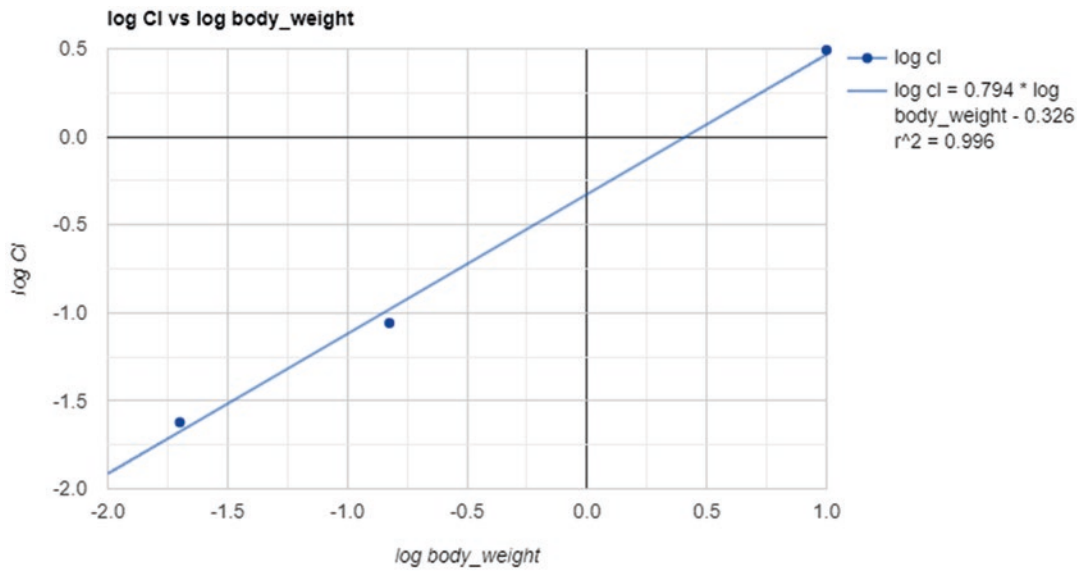

Fig. 7.10 Interspecies scaling using pharmacokinetic data obtained after an intravenous administration of a drug in the mouse, rat, and dog

Table 7.11 Human predicted parameters based on interspecies scaling using the body weight analysis

Dose (mg/kg)	Kel (1/hr)	Body weight (kg)	Body surface area (m^2)	$T_{1/2}$ (hr)	$AUC_{0-\infty}$ (mg/L·hr)	Cl/F (L/hr)	V_d/F (L)	C_{max} (mg/L)	T (hr)	C_{avg} (mg/L)
1	0.156	60	1.62	4.45	4.93	12.17	78.1	0.77	12	0.41

Table 7.12 HED based on the animal NOAEL

Species	NOAEL (mg/kg)	HED factor	HED (mg/kg)
Mouse	100	12.3	8.1
Rat	75	6.2	16.1
Dog	50	1.8	55.6

can be customized by changing a factor. Using the maximum safe recommended dose (MSRD) of 10 mg/kg and using the eight steps, the dose escalation is computed. The initial dose value can be selected as 1/10 of MSRD or other as appropriate.

16 Compartmental Pharmacokinetics (CA-PK)

The plasma concentration vs. time data after administration of a drug can be fitted to the appropriate pharmacokinetic model depending on the route of administration to the following compartmental body models (CBM) [2] as shown in Table 7.14:

The concentration and time data is fitted to a selected model, and the convergence of parameters is achieved by Levenberg-Marquardt method [13], with selected weighting options (1, $1/C_{obs}$, $1/C^2_{obs}$, $1/C_{pred}$, and $1/C^2_{pred}$). The parameters, their standard errors, secondary parameters, and model selection criteria are computed (Table 7.15), and the observed and predicted concentration plots are shown in Fig. 7.11.

17 Pharmacodynamics (PD) Analysis

Pharmacodynamics is a relationship between the plasma concentration of a drug and a given response [2]. The response can be the drug interaction with the receptor both directly and reversibly (e.g., antiarrhythmic and neuromuscular blocking agents), indirectly (e.g., coumarin anticoagulants), or irreversibly binding to the receptors (e.g., anticancer agents and bactericidal antibiotics).

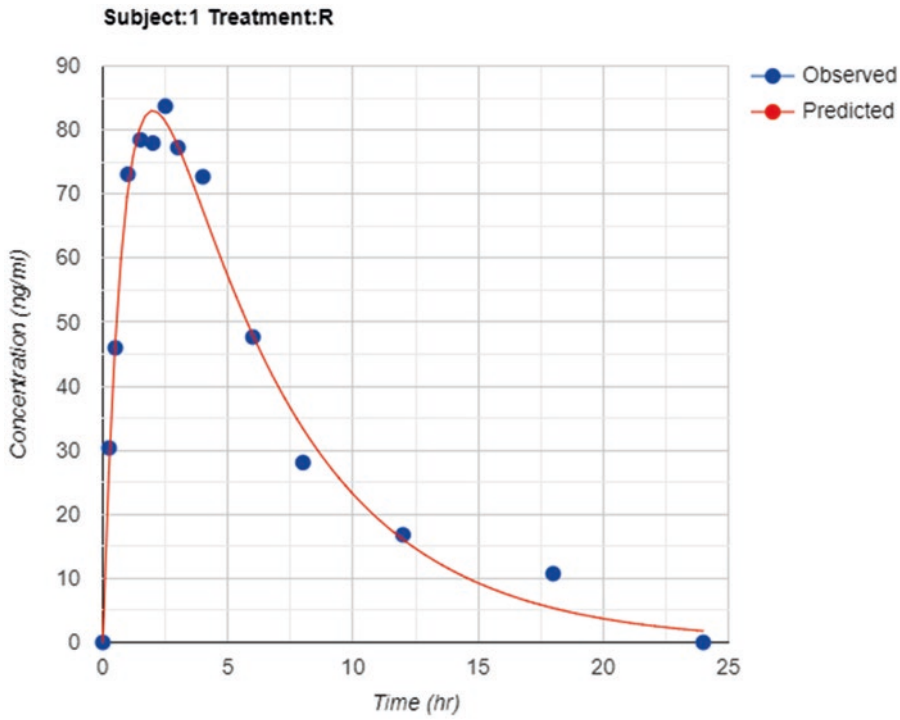

Fig. 7.11 Plot of the observed and predicted concentrations for a 1-CBM oral absorption model

Table 7.13 Dose escalation scheme based on the NOAEL and MSRD

	Empiric		Modified-Fibonacci		Logarithmic	
Dose no.	Factor	Dose value	Factor	Dose value	Factor	Dose value
1	1	1	1	1	0	1
2	2	2	0.65	1.7	0.5	1.6
3	1.5	3	0.52	2.5	1	2.7
4	1.3	3.9	0.4	3.5	1.5	4.5
5	1.3	5.1	0.29	4.5	2	7.4
6	1.3	6.6	0.33	6	2.5	12.2
7	1.2	7.9	0.33	8	3	20.1
8	1.1	8.7	0.33	10.7	3.5	33.1

Using a 10 mg/kg MSRD and the eight steps, the dose escalation is computed. The initial dose value is selected as 1/10 of MSRD

The following pharmacodynamic models are available for evaluation of concentration-effect relationship after a drug administration (Table 7.16). The effect vs. concentration data is optimized using Levenberg-Marquardt or Nelder-Mead [14] methods, and the parameter estimate, standard error, percent coefficient of error, and model diagnostics are computed. An example of a model fit for the sigmoidal E_{max} model is presented in Table 7.17 and Fig. 7.12.

18 Dissolution Data Analysis

Dissolution is the process of dissolving a drug substance from the solid state. Drug absorption from a solid dosage form after oral administration depends on the release of the drug substance from the drug product, the dissolution of the drug under physiological conditions, and the absorption across the gastrointestinal tract. Because of the critical nature of the first two of these steps, in vitro dissolution may be relevant to the prediction of in vivo performance of drug product. Therefore, in vitro dissolution for immediate release solid oral dosage forms, such as tablets and capsules, is used to assess the lot-to-lot quality of a drug product, guide development of new formulations, and ensure continuing product quality and performance after certain changes,

Table 7.14 Compartmental analysis models and equations

Route of administration	PK model	Equation
Extravascular 1-CBM (with and without lag time)	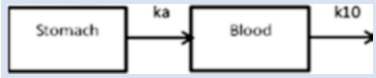	$C = \frac{FDka}{V(ka-k10)}\left[e^{-(k10.t)} - e^{-(ka.t)}\right]$ C concentration, F bioavailability, D dose, V/F apparent oral volume of distribution, ka first-order absorption rate constant, $k10$ first-order elimination rate constant
2-CBM (with and without lag time)	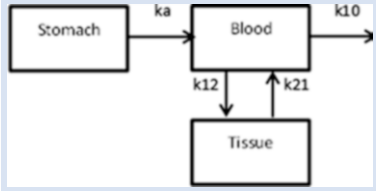	$Cp = Ae^{-\propto t} + Be^{-\beta t} + Ce^{-kat}$ $A = \frac{kaFD(k21-\propto)}{V(ka-\propto)(\beta-\alpha)}$ $B = \frac{kaFD(k21-\beta)}{V(ka-\beta)(\alpha-\beta)}$ $C = \frac{kaFD(k21-ka)}{V(\alpha-ka)(\beta-ka)}$
IV bolus 1-CBM		$C = \frac{D}{V}e^{-k10.t}$
2-CBM	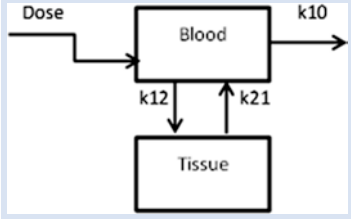	$C = Ae^{-\propto t} + Be^{-\beta t}$ $A = \frac{D(\propto -k21)}{V(\alpha-\beta)}$ $\alpha + \beta = k12 + k21 + k10$ $\alpha\beta = k21k10$ $B = \frac{D(k21-\beta)}{V(\alpha-\beta)}$
3-CBM	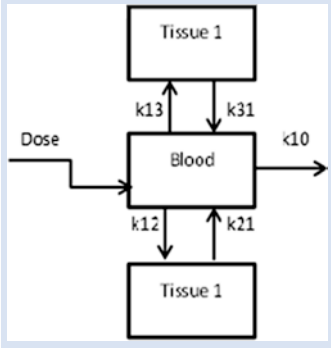	$Cp = Ae^{-\propto t} + Be^{-\beta t} + Ce^{-\gamma t}$ $A = \frac{D(k21-\alpha)(\alpha-k31)}{V(\gamma-\alpha)(\alpha-\beta)}$ $Co = A + B + C$ $B = \frac{D(k21-\beta)(k31-\beta)}{V(\gamma-\beta)(\alpha-\beta)}$ $C = \frac{D(k21-\gamma)(k31-\gamma)}{V(\gamma-\alpha)(\gamma-\beta)}$
IV infusion 1-CBM	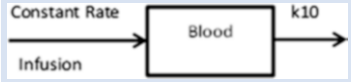	$C = \frac{ko}{Vk10}\left(1-e^{-k10T}\right)e^{-k10t*}$

(continued)

Table 7.14 (continued)

Route of administration	PK model	Equation
2-CBM	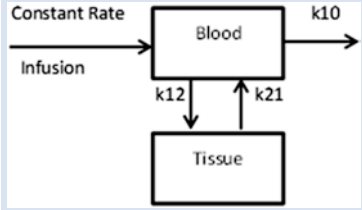	$C = \frac{ko(k21-\alpha)(e^{-\alpha T}-1)}{V\alpha(\alpha-\beta)}e^{-\alpha t^*} + \frac{ko(\beta-k21)(e^{-\beta T}-1)}{V\beta(\alpha-\beta)}e^{-\beta t^*}$
3-CBM	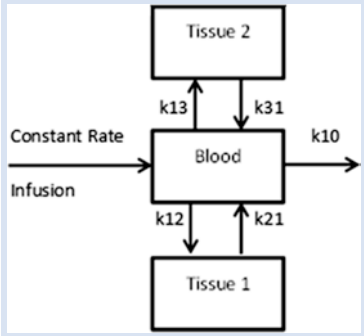	$Cp = A\left[e^{(\alpha t^*)} - e^{(-\alpha T)}\right] + B\left[e^{(-\beta t^*)} - e^{(-\beta T)}\right] + C\left[e^{(-\gamma t^*)} - e^{(-\gamma T)}\right]$

Table 7.15 Parameters of a 1-CBM oral absorption model

Parameter	Unit	Estimate	Standard error	CV%
Subject 1				
A	ng/ml	144.532	3.715	2.57
ka	1/hr	164	031	2.946
*k*10	1/hr	0.183	005	2.63
$t_{1/2}ka$	hr	0.651		
$t_{1/2}k10$	hr	3.787		
V/*F*	(mg)/(ng/ml)	0.836		
CL/*F*	(mg)/(ng/ml)hr	0.153		
T_{max}	hr	1.997		
C_{max}	ng/ml	8329		
AUC_{0-t}	ng/ml*hr	64448		
AUC_{0-inf}	ng/ml*hr	653.81		
AUMC	ng/ml*hr^2	418666		
MRT	hr	6.403		
$R_{obs\text{-}pre}$	–	0.995		
SS	–	14128		
WSS	–	14228		
R^2	–	0.997		
WR^2	–	0.997		
SE	–	3.593		
AIC	–	75.384		
SC	–	77.301		

such as changes in the formulation, the manufacturing process, the site of manufacture, and the scale-up of the manufacturing process [15, 16]. The mathematical models for describing dissolution models [17–20] for drugs are shown in Table 7.18.

An example of a dissolution data fitted to the Weibull_4 model is shown in Table 7.19 and Fig. 7.13.

19 Dissolution Profile Comparison

Dissolution profile comparison is done to accept product sameness under scale-up and post-approval-related changes, to waive bioequivalence requirements for lower strengths of a dosage form, and to support waivers for other bioequivalence requirements [15, 16, 19]. The following are dissolution profile comparison using model-independent methods.

20 Difference Factor

The difference factor calculates the percent difference between the two curves at each time point and is a measurement of the relative error between the two curves:

$$f1 = \frac{\left[\sum_{t=1}^{n} \| Rt - Tt \|\right]}{\left[\sum_{t=1}^{n} Rt\right]} * 100 \tag{7.20}$$

where

Rt = reference assay at time point t
Tt = test assay at time point t
n = the number of dissolution time points

The dissolution data is displayed in Fig. 7.14, and the $f1$ comparison analysis is shown in Table 7.20.

21 Similarity Factor

The similarity factor is a logarithmic reciprocal square root transformation of the sum squared error and is a measurement of the similarity in the percent dissolution between the two curves:

$$f2 = 50 * \log\left\{\left[1 + \left(1/n\right)\sum_{n}^{t=1}\left(Rt - Tt\right)^2\right]^{-0.5} * 100\right\} \tag{7.21}$$

where

Rt = reference assay at time point t
Tt = test assay at time point t
n = the number of dissolution time points

The dissolution data is displayed in Fig. 7.14, and the $f2$ comparison analysis is shown in Table 7.21. A bootstrap analysis for the $f2$ comparison can also be performed, and the results are displayed in Table 7.21.

22 Multivariate Statistical Difference (MSD) Determination

In instances where dissolution is measured at multiple time points and within batch variation is more than 15% CV, a multivariate model-independent procedure is more suitable for dissolution profile comparison [21]. The statistic of Mahalanobis distance is used to assess the difference between the means of test and reference data with adjustments for differences in measurement variation at different time points and the correlation among the measurements at multiple time points. The variance-covariance matrix and inverse of variance-covariance matrix for the pooled data is computed to calculate overall statistics as shown in Table 7.22.

23 IVIVC Model

The objective of developing an in vitro–in vivo correlation (IVIVC) is to establish a predictive mathematical model describing the relationship between an in vitro property and a relevant in vivo response [22]. The IVIVC for modified release dosage forms has often been used during pharmaceutical development in order to reduce development time and optimize the formulation. A good correlation is a tool for predicting in vivo results based on in vitro data. IVIVC allows dosage form optimization with the fewest possible trials in human, fixes dissolution acceptance criteria, and can be used as a surrogate for further bioequivalence studies; furthermore, it is also recommended by regulatory authorities. The schematic of the process to develop an IVIVC is shown in Fig. 7.15. It involves in vitro dissolution data for formulations under evaluation and in vivo bioavailability data for formulations, as well as a reference formulation such as intravenous, solution, or immediate release formulation [20, 23–30]. The correlations are established between in vivo parameters and in vitro data.

Table 7.16 Pharmacodynamics models and equations

Model	Equation
E_{max}	$E = \frac{E_{max}.C}{C + EC_{50}}$
E_{max} with baseline effect	$E = E_0 + \frac{(E_{max} - E_0).C}{C + EC_{50}}$
Sigmoid E_{max}	$E = \frac{E_{max}.C^{\gamma}}{C^{\gamma} + EC_{50}{}^{\gamma}}$
Sigmoid E_{max} with baseline effect	$E = E_0 + \frac{(E_{max} - E_0).C^{\gamma}}{C^{\gamma} + EC_{50}{}^{\gamma}}$
Inhibition E_{max}	$E = E_{max}\left[1 - \left(\frac{C}{C + EC_{50}}\right)\right]$
Inhibition E_{max} with baseline effect	$E = E_{max} - (E_{max} - E_0)\left(\frac{C}{C + EC_{50}}\right)$
Inhibition sigmoid E_{max}	$E = E_{max}\left[1 - \left(\frac{C^{\gamma}}{C^{\gamma} + EC_{50}{}^{\gamma}}\right)\right]$
Inhibition sigmoid E_{max} with baseline effect	$E = E_{max} - (E_{max} - E_0)\left(\frac{C^{\gamma}}{C^{\gamma} + EC_{50}{}^{\gamma}}\right)$

E effect, E_{max} maximum effect, E_0 baseline, *C* concentration, EC_{50} concentration producing 50% of maximum effect, γ sigmoidicity factor

24 Level A Correlation

A level A correlation is a predictive mathematical model for the relationship between the entire in vitro dissolution-time course and the entire in vivo response-time course of drug absorbed. A level A IVIVC is considered to be the most informative and is recommended [22]. It involves obtaining in vitro dissolution profiles and in vivo plasma concentration profiles for the formulations under evaluation. The estimate of the in vivo absorption, or dissolution time course, using a deconvolution technique described below for each formulation and subject is obtained. The linear correlation, as shown in Fig. 7.15d, between the % absorbed and the % dissolved to predict plasma concentrations is achieved using the convolution methods. The predictability in the model is determined by estimation of the prediction error in AUC and C_{max} for internal and/or external batches of formulations based on observed and predicted plasma concentration-time data [22]:

Table 7.17 PD parameter estimates for a sigmoidal E_{max} model

Parameter	Estimate	Standard error	CV%
Subject 1			
E_{max}	99.995	3.948	3.948
EC_{50}	11.424	0.846	7.406
Gamma	1.371	0.125	9.127
Diagnostics	Values		
$r_{obs\text{-}pre}$	0.998		
SS	14.719		
WSS	14.719		
R^2	1		
WR^2	1		
SE	1.918		
AIC	24.824		
SC	24.662		

$$\%PE = \left(\frac{\text{observed} - \text{predicted}}{\text{observed}}\right) * 100 \tag{7.22}$$

Average absolute percent prediction error (%PE) of 10% or less for C_{max} and AUC establishes the predictability of the IVIVC. In addition, the %PE for each formulation should not exceed 15%.

The following models are included for deconvolution of in vivo data in PKMP for analysis:

24.1 Deconvolution: Wagner-Nelson Method

For a drug with one-compartment body model characteristics, the fraction of drug absorbed to time t is given by [2]:

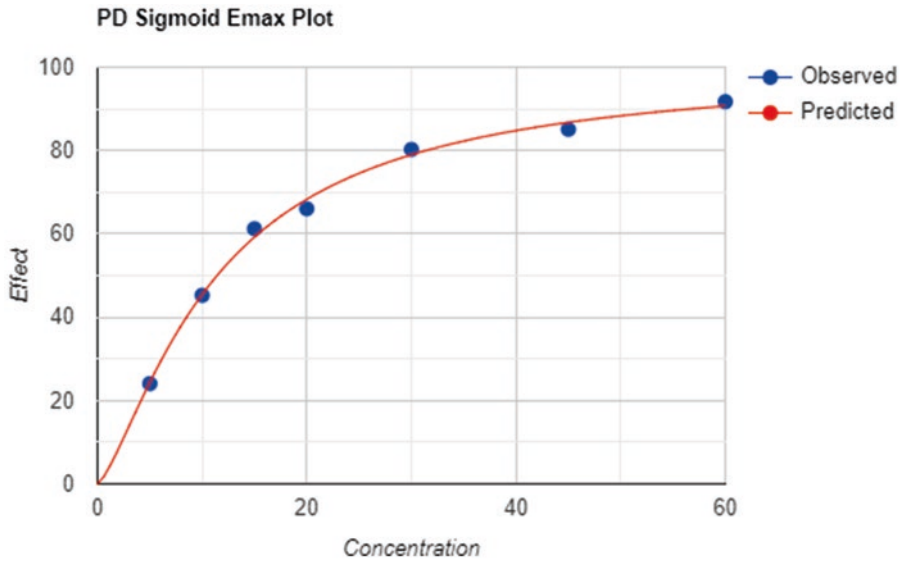

Fig. 7.12 Plot of the observed and predicted effect vs. concentration plots for a sigmoid E_{max} model

$$\frac{(X_A)_t}{(X_A)_\infty} = \frac{C_t + K\int_0^t Cdt}{K\int_0^\infty Cdt} \tag{7.23}$$

X_A = amount of drug absorbed to time t or ∞
C_t = plasma concentration of drug at time t
K = apparent first-order elimination rate constant

24.2 Convolution

Using the superposition principle and following equation for 1-CBM [25], the amount of a drug in the body is predicted from the amount dissolved at each time and K and summed over all the individual dissolution times:

$$X = X0e^{-Kt} \tag{7.24}$$

$X0$ = amount in at each dissolution time
K = apparent first-order elimination rate constant

Predicted concentrations (Cp) are obtained as X:

$$Cp_{\text{pred}} = \frac{X}{V_d \text{ or } S_F} \tag{7.25}$$

V_d = apparent volume of distribution
S_F = scaling factor

24.3 Deconvolution: Loo-Riegelman Method

For a drug with two-compartment body model characteristics, the fraction of drug absorbed to time t is given by [2]:

$$\frac{(X_A)_t}{(X_A)_\infty} = \frac{C_t + k10\int_0^t Cdt + \left(1/V_c\right)(X_p)_t}{k10\int_0^\infty Cdt} \tag{7.26}$$

X_A = amount of drug absorbed to time t or ∞
C_t = plasma concentration of drug at time t
$k10$ = apparent first-order elimination rate constant from the central compartment
V_c = the apparent volume of the central compartment

Table 7.18 Dissolution models

Model	Definition	Equation
Zero order	F = amount of drug dissolved in time t $k0$ = zero-order release constant	$F = k0.\ t$
Zero order with T_{lag}	T_{lag} = lag time in dissolution	$F = k0.\ (t - T_{lag})$
Zero order with $F0$	$F0$ = initial amount of drug in the solution	$F = F0 + k0.\ t$
Baker-Lonsdale	k_{BL} = release rate constant	$\frac{3}{2}\left[1-\left(1-\frac{F}{100}\right)^{\frac{2}{3}}\right]-\frac{F}{100}=k_{BL}t$
Baker-Lonsdale with T_{lag}		$\frac{3}{2}\left[1-\left(1-\frac{F}{100}\right)^{\frac{2}{3}}\right]-\frac{F}{100}=k_{BL}\left(t-T_{lag}\right)$
First order	k = first-order rate constant	$F = 100.\ (1 - e^{-k.\ t})$
First order with T_{lag}		$F=100.\left[1-e^{-k.\left(t-T_{lag}\right)}\right]$
First-order with T_{lag} F_{max}	F_{max} = maximum amount of drug dissolved in time t	$F=F_{max}.\left[1-e^{-k.\left(t-T_{lag}\right)}\right]$
First-order with F_{max}		$F = F_{max}.\ [1 - e^{-k.\ t}]$
Higuchi	K_H = Higuchi dissolution constant	$F = K_H.\ t^{0.5}$
Higuchi $F0$		$F = F0 + K_H.\ t^{0.5}$
Higuchi with T_{lag}		$F = K_H.\ (t - T_{lag})^{0.5}$
Hixson-Crowell	K_{HC} = constant	$F = 100.\ [1 - (1 - K_{HC}.\ t)^3]$
Hixson-Crowell with T_{lag}		$F = 100.\ [1 - (1 - K_{HC}.\ (t - T_{lag})^3]$
Hopfenberg	K_{HB} = constant	$F = 100.\ [1 - (1 - K_{HB}.\ t)^n]$
Hopfenberg with T_{lag}		$F = 100.\ \{1 - [1 - K_{HB}.\ (t - T_{lag})]^n\}$
Korsmeyer-Peppas	F = fraction drug released at time t K_{KP} = release rate constant n = release exponent	$F = K_{KP}.\ t^n$
Korsmeyer-Peppas with $F0$		$F = F0 + K_{KP}.\ t^n$
Korsmeyer-Peppas with T_{lag}		$F = K_{KP}.\ (t - T_{lag})^n$
Weibull_1	α = scale parameter T_i = location of parameter β = shape parameter	$F=100.\left[1-e^{-\frac{(t-T_i)^{\beta}}{\propto}}\right]$
Weibull_2		$F=100.\left[1-e^{-\frac{(t)^{\beta}}{\propto}}\right]$
Weibull_3		$F=F_{max}.\left[1-e^{-\frac{(t)^{\beta}}{\propto}}\right]$
Weibull_4		$F=F_{max}.\left[1-e^{-\frac{(t-T_i)^{\beta}}{\propto}}\right]$

Table 7.19 Weibull_4 parameters for a dissolution data shown in Fig. 7.13

$F = F_{max}$.{1−Exp[−((*t*−*Ti*)^beta)/alpha]}			
Parameter	Value		
Alpha	188.547		
Beta	1.212		
Ti	119.829		
F_{max}	2.547		
Parameter (time for % dissolved)		Value	
*T*25		25.323	
*T*50		47.97	
*T*75		7881	
*T*80		7733	
*T*90		84.354	
Parameter		Value	
N_observed		8	
DF		4	
R_obs-pre		0.996	
Rsqr		0.991	
Rsqr_adj		0.991	
MSE		19.878	
MSE_root		4.458	
Weighting		1	
SS		79.511	
WSS		79.511	
AIC		3707	
MSC		4.476	

X_p = amount of drug in the peripheral compartment

24.4 Convolution

Using the superposition principle, drug amounts in the body are predicted from the dissolution amount at each time and using the following 2-CBM equation:

$$X = \frac{X0(\alpha - k21)}{(\alpha - \beta)} e^{-\alpha t} + \frac{X0(k21 - \beta)}{(\alpha - \beta)} e^{-\beta t} \tag{7.27}$$

Predicted concentrations (*Cp*) are obtained as

$$Cp_{pred} = \frac{X}{V_c \text{ or } S_F} \tag{7.28}$$

V_c = apparent volume of distribution of central compartment

S_F = scaling factor

24.5 Numeric Deconvolution

The absorption rate (r_{abs}) that results in plasma concentration $c(t)$ can be estimated by solving the following equation:

$$c(t) = \int_t^0 c_\delta (t-u) r_{abs}(u)\, du \tag{7.29}$$

where

$c(t)$ = plasma concentration versus time profiles of tested formulation

C_δ = concentration time profile resulting from instantaneous input of a unit amount of drug

r_{abs} = input rate of the oral solid dosage form into the body

u = variable of integration

25 Correlations

25.1 Level A Correlation

Using an Interpolation Method

Slope and intercept between two successive time points for mean %dissolution vs. time and mean % in vivo fraction absorbed (FA) vs. time are computed. Times of 10%, 20%, and up to 100% dissolution are determined, and the %FA corresponding to these times is computed. Based on the %FA vs. %dissolved data, level A linear regression with parameters slope, intercept, and correlation coefficient is obtained.

Using the Hill Equation

$$D = \frac{D_{max}[C]^\gamma}{[D_{50}]^\gamma + [C]^\gamma} \tag{7.30}$$

D = rate of dissolution

D_{max} = maximum dissolution rate

C = %dissolved

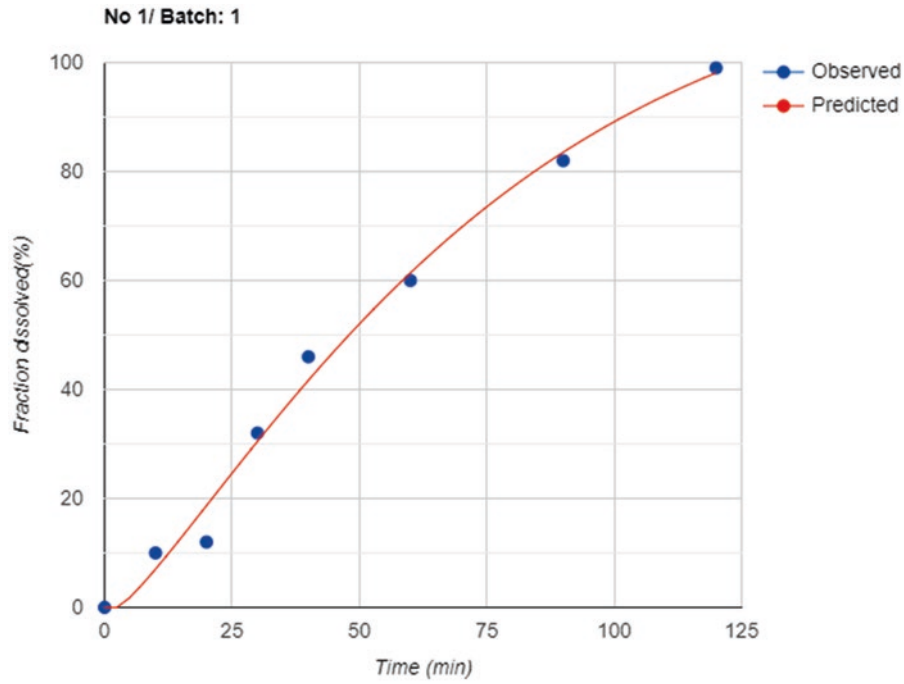

Fig. 7.13 Plot of the observed and predicted dissolution data fitted to a Weibull_4 model

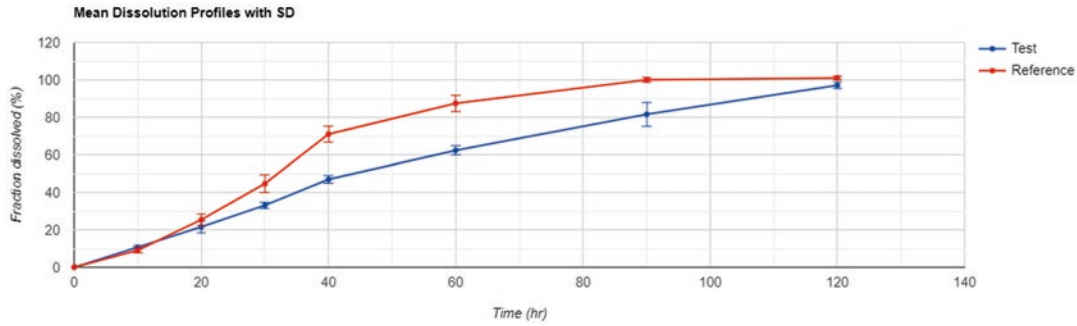

Fig. 7.14 Mean (± SD) dissolution profiles for test and reference oral products

D_{50} = time of 50% dissolved
γ = shape factor

Both %dissolution-time and %FA-time data are fitted to the Hill equation. Additional computations are done in the same way, as indicated in the interpolation method above.

Using Weibull Equation

$$D = D_{\max} * \left\{ 1 - e^{\left[-\frac{(t-Ti)^{\beta}}{\alpha} \right]} \right\} \quad (7.31)$$

D = cumulative % dissolved
t = time
α = scale parameter
Ti = lag time

Table 7.20 *f*1 difference factor in dissolution comparison

	Mean_*R* vs Individual_*T*		Mean_Test vs Mean_Reference
Overall statistics	Mean	SE	
*f*1	25.2	0.93	25.1
Is *f*1 between [0,15] for Mean_Test and Mean_Reference?	No		
Similarity of test and reference	Reject		

Table 7.21 *f*2 difference factor in dissolution comparison and the bootstrap simulation

	Mean_*R* vs Individual_*T*		Mean_Test vs Mean_Reference
Overall statistics	Mean	SE	
f2	41.5	0.73	41.7
Is *f*2 between [50,100] for Mean_Test and Mean_Reference?	No		
Similarity of test and reference	Reject		
Bootstrap analysis statistics for *f*2	Value		
Observed *f*2	41.7		
Number of bootstrap	5000		
Bootstrap mean	41.7		
Bootstrap median	41.7		
5% percentile	40.1		
95% percentile	43.3		
Skewness	0.1		
Kurtosis	0		

B = shape parameter

For further computations, a similar process, as described above under using Hill equation, is applied.

25.2 Level B Correlation

The level B correlation is a predictive mathematical model for the relationship between summary parameters characterizing the in vitro and in vivo time courses, such as the mean in vitro dissolution time to the mean in vivo dissolution time, the mean in vitro dissolution time to the mean residence time in vivo, or the in vitro dissolution rate constant to the absorption rate constant [22]. An example of mean dissolution time in vivo and mean dissolution time analysis is shown in Fig. 7.16.

25.3 Level C Correlation

The level C correlation is a predictive mathematical model of the relationship between the amounts dissolved in vitro at a particular time (t50%, t90%, etc.) and a summary parameter characterizing the in vivo time course (AUC, T_{max}, or C_{max}) [22]. An example of level C correlation for the C_{max} for three formulations and % dissolved at time is shown in Fig. 7.17.

26 Simulation

Simulation analysis allows predicting dose-concentration, as well as concentration-response relationships, based on mathematical models. Pharmacokinetic simulations allow predicting multiple-dose drug concentrations based on a single-dose data which can be used to evaluate safe margins during drug development. In formulation development,

Table 7.22 Overall statistics for a MSD analysis

Statistics	Value
P (sampling points)	8
K (scaling factor)	0.511
F (*p*, *n*1 + *n*2–*p*–1, 0.95)	2.641
Hotelling's T^2	1533.549
Mahalanobis distance (MSD)	15.987
Relative distance(RD)	23.717
Lower 95% CR MSD	13.715
Upper 95% CR MSD	18.26
Upper 95% CI less than RD	Yes
Reference and test global similarity	Reject

IVIVC simulations aid in modified release product optimization. Pharmacodynamic simulations allow examining the relationship between the drug concentration and the response. These techniques assist in optimizing the formulation development and predicting the dose-response relationship to design better clinical trials.

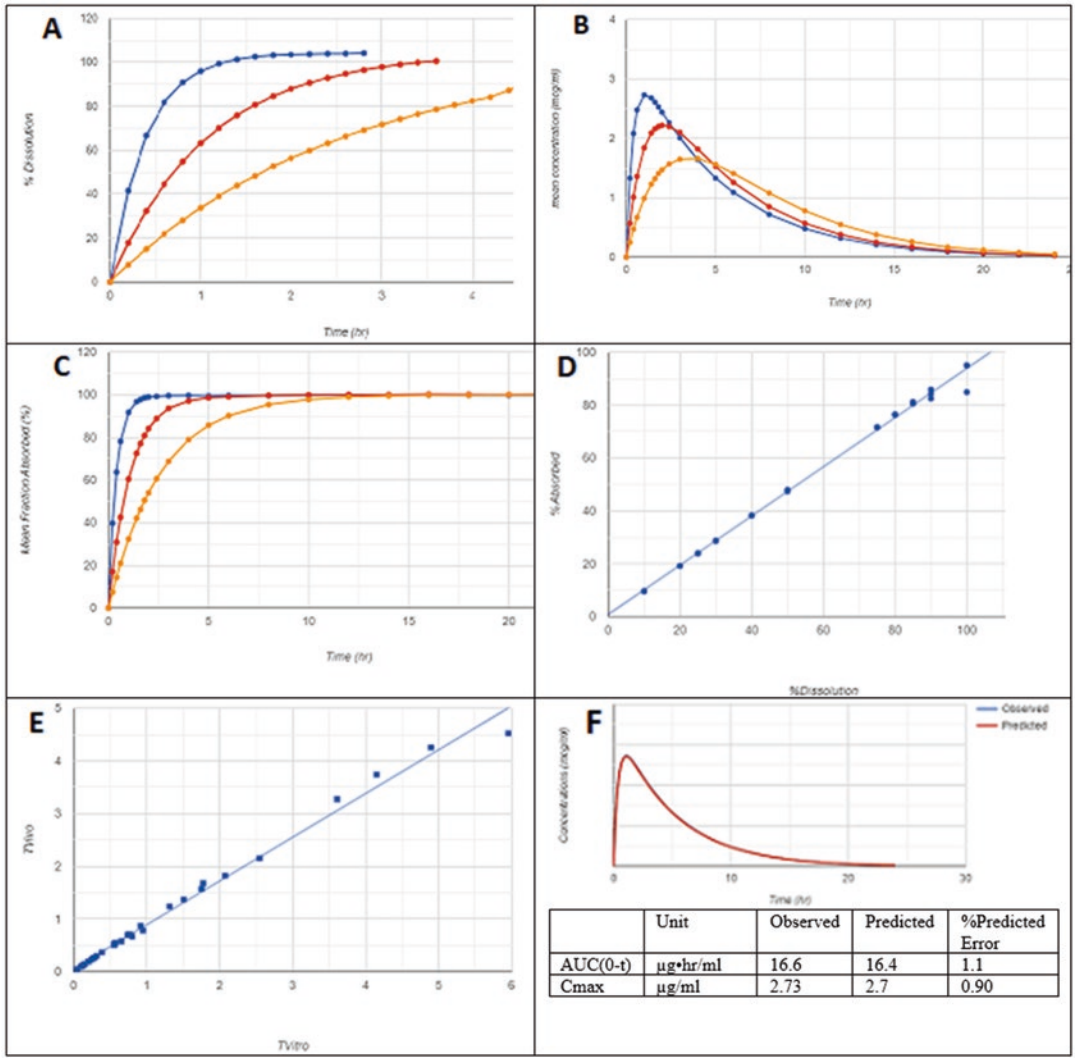

	Unit	Observed	Predicted	%Predicted Error
AUC(0-t)	µg•hr/ml	16.6	16.4	1.1
Cmax	µg/ml	2.73	2.7	0.90

Fig. 7.15 Schematic representation of the process to develop an IVIVC involving (**a**) dissolution, (**b**) in vivo concentration data, (**c**) computation of in vivo dissolution or fraction absorbed, (**d**) level A correlation for in vivo dissolution and in vitro dissolution, (**e**) Levy plot related to time for in vivo dissolution and time for in vitro dissolution, and (**f**) prediction error for convolution

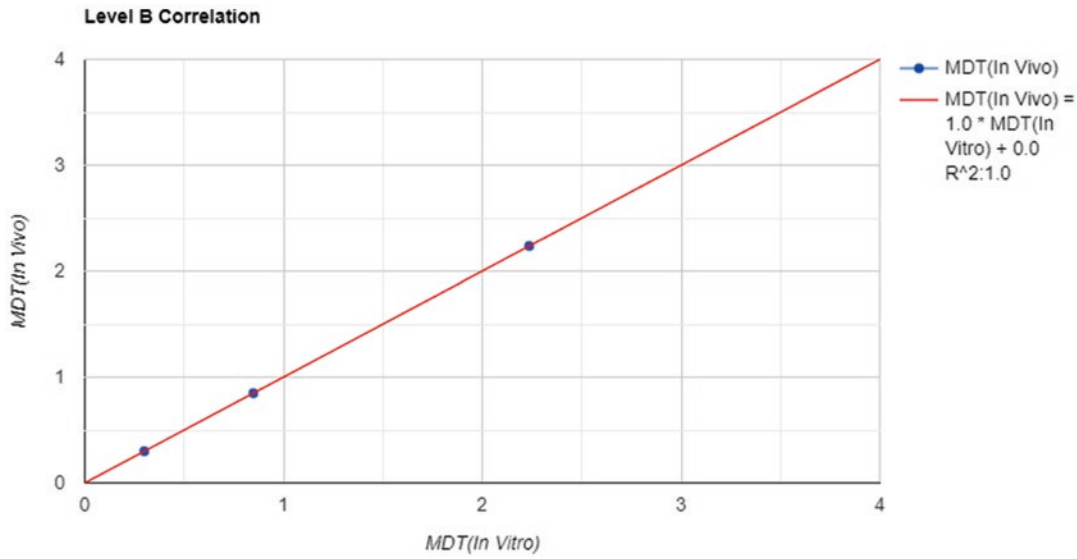

Fig. 7.16 Level B correlation for MDT (in vivo) and MDT (in vitro)

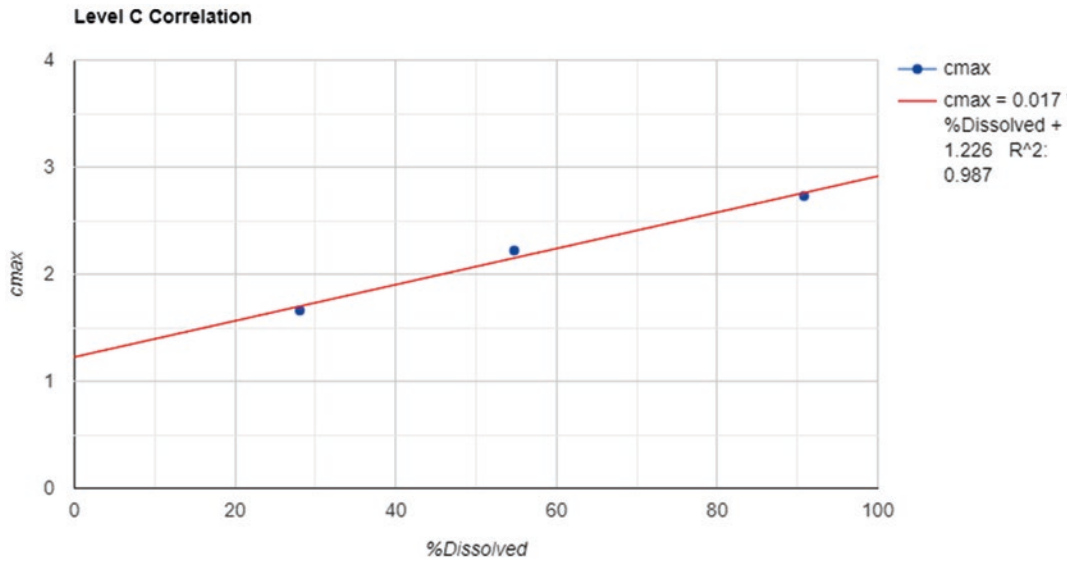

Fig. 7.17 Level C correlation for C_{max} and % dissolved at a time for three formulations

26.1 Pharmacokinetic Simulation

Pharmacokinetic simulations can be performed for single and multiple doses based on explicit equations as shown in Table 7.14 for 1-CBM, 2-CBM, and 3-CBM models for oral, IV bolus, or IV infusion. An example of a 1-CBM oral multiple dosing is shown in Fig. 7.18.

26.2 Pharmacodynamic Simulation

Pharmacodynamic simulations can be performed based on explicit equations as shown in Table 7.16, and an example of the simulation for inhibitory E_{max} model is shown in Fig. 7.19.

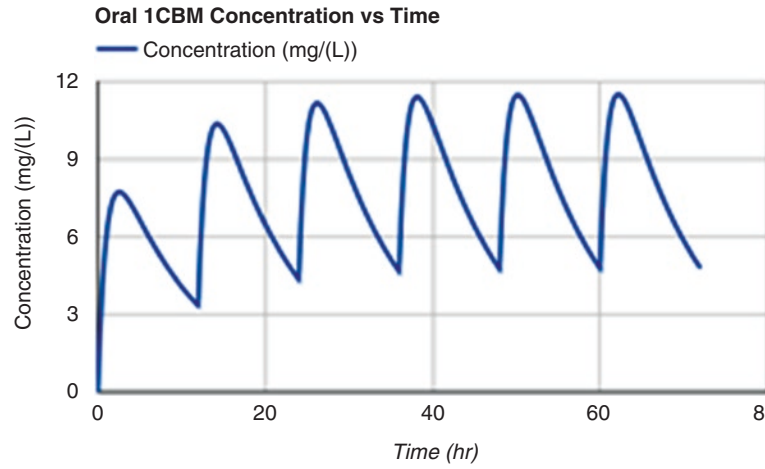

Fig. 7.18 Simulation of multiple oral doses for a 1-CBM using Ke, 0.1 (/hr); *Ka*,1.0 (/hr); V_d, 10 (L); tau, 12 hr; dose, 100 mg; number of doses, 6; and step size, 0.25

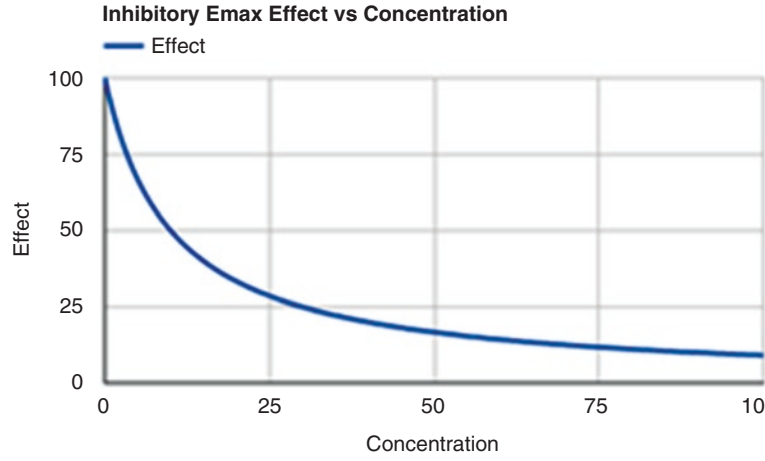

Fig. 7.19 Simulation plot of the effect vs. concentration for an inhibitory E_{max} model using E_{max}, 100%; EC_{50}, 10 (ng/mL); *Cp* (initial-final), 0–100 ng/mL; and step size, 0.5

27 IVIVC

Typically, in a formulation development, dissolution data becomes available as the first step. The data can be fitted to dissolution models such as E_{max} or Weibull functions. If the PK disposition parameters after intravenous administration, such as C0 and Kel for a 1-CBM or A, α, B, and β for a 2-CBM, are available from a study or the literature, then using the convolution integral, as shown in Eq. (7.29), can be used to predict the concentrations as a product of input rate and disposition function. In Fig. 7.20, dissolution data is shown, fitted to an E_{max} model, and the model parameters are displayed. The disposition parameters, C_0 and Kel, for a 1-CBM, following IV bolus administration, are used to simulate the predicted concentrations as shown in Fig. 7.20. The concentration-time data obtained from this simulation can be further evaluated for NCA analysis, and bioequivalency simulation can be performed with the knowledge of variability, as determined by SD or CV%.

28 Bioequivalence (BE)

The concentration-time data with a measure of variability, such as SD or CV% for two treatments (Table 7.23), can be simulated using the bootstrap method. The pharmacokinetic parame-

Time (min)	%Dissolved
0	0
10	10
20	12
30	32
40	46
60	60
90	82
120	99

1 CBM IV Parameters:		
C0 (µg/L)	K10 (/min)	
10	1	
Hill parameters:		
Emax	EC50	Gamma
144.2	72.7	1.5

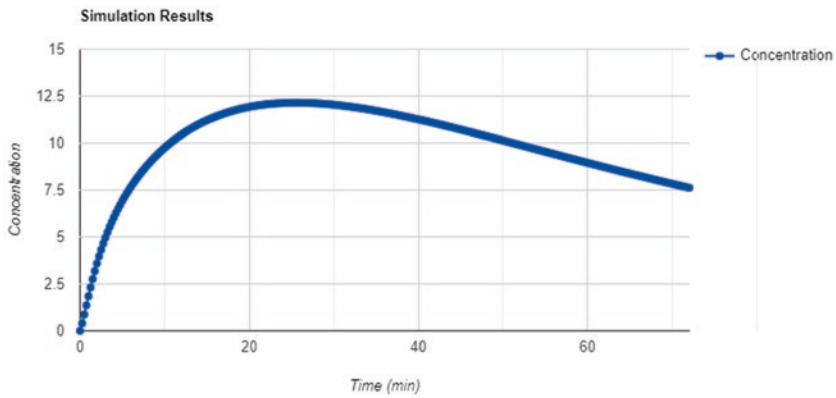

Fig. 7.20 Simulation of an IVIVC using the dissolution data and disposition parameters for a drug

Table 7.23 Observed and the bootstrap simulated concentration-time data for BE simulation

Treatment	Time (hr)	*Cp* observed	SD observed	*Cp* simulation	SD simulation	Count
Test	0	0	0	0	0	500
Test	0.5	2.685	2.333	2.821	2.18	500
Test	1	6.577	3.19	6.55	3.237	500
Test	1.5	6.825	2.136	6.632	2.247	500
Test	2	7.16	2.77	7.36	2.231	500
Test	Additional data					

ters such as AUC and C_{max} and confidence intervals (90, 95, or 99%) are calculated. The user can compare the AUC and C_{max} ratios for test and reference formulations to estimate bioequivalence (Table 7.24).

29 Sample Size

For bioequivalence studies using a standard two-treatment crossover design, the sample size needs to be selected with the power to demonstrate the test and reference ratio for averages of C_{max}, and AUC is within an 80–125% limit. The sample size is calculated using within-subject variability (SD) for the PK parameter, magnitude of subject-by-formulation interaction, the difference of the arithmetic means of the log transformed parameters (delta, usually taken as 0.05), and the 80% or 90% power [6, 31]. The sample size calculations are calculated as below and shown in Table 7.25:

$$N \geq \frac{2\left[t\left(\alpha, df = N' - 2\right) + t\left(\beta, df = N' - 2\right)\right]^2 * \left(2\sigma w^2 + \sigma D^2\right)}{\left(\ln\left(\theta\right) - \ln\left(1 - \quad\right)\right)^2}$$

where

Table 7.24 Bootstrap AUC and C_{max} and 90% confidence interval estimates

Treatment	Scale	Parameter	Count	Mean	SD	CV%	90% CI lower	90% CI upper
Test	Original	AUC	500	189.6	12.9	6.8	188.4	190.7
		C_{max}	500	21.7	3.0	13.7	21.5	22
	Natural logarithm	AUC	500	5.2	0.1		5.2	5.2
		C_{max}	500	3.1	0.1		3.1	3.1
Reference	Original	AUC	500	190.9	13.1	6.9	189.7	192
		C_{max}	500	21.9	3.1	14.2	21.6	22.2
	Natural logarithm	AUC	500	5.2	0.1		5.2	5.3
		C_{max}	500	3.1	0.1		3.1	3.1

Table 7.25 Sample size calculations for a two-period, two-sequence, two-treatment crossover BE study for alpha (one-sided) = 0.05, delta = 0.05, and BE margin = 0.8

		Power	
sigma_*w*	sigma_*d*	80%	90%
01	0.15	6	8
0.1	0.15	12	14
0.15	0.15	16	22
01	0.23	12	18
0.1	0.23	18	24
0.15	0.23	22	30
01	0.3	20	28
0.1	0.3	24	34
0.15	0.3	30	42
01	0.5	54	74
0.1	0.5	58	80
0.15	0.5	64	88

$$N' \geq \frac{2\left[Z\alpha + Z\beta\right]^2 * \left(2\sigma w^2 + \sigma D^2\right)}{\left(\ln\left(\theta\right) - \ln\left(1 - \quad\right)\right)^2}$$

sigma_*w* (σw) = within-subject variability (standard deviation) for the PK parameter
sigma_*D* (σD) = subject-by-formulation interaction for the PK parameter
Delta (Δ) = deviation from a perfect equivalence, 1-delta rather than 1, recommended 0.05
Power (β) = 80% or 90%
Alpha (α) = one-sided 5%, it is fixed according to regulatory convention.
BE margin (θ) = 0.8
Df = degrees of freedom

30 Differential Equation-Based Analysis (dEq)

30.1 Predefined Simulation Models

Differential equation-based analysis is a powerful tool to simulate PK/PD data. The predefined differential equations for pharmacokinetic 1-, 2-, and 3-CBM for extravascular, IV bolus, IV infusion (Table 7.14), and PD models (Table 7.16) are included, allowing simultaneous prediction of single- and multiple-dose PK/PD analysis. Additionally, an effect compartment [2] can be included in the PD analysis. The integration is performed using either by Runge-Kutta (4th order), Runge-Kutta-Cash-Karp, or Runge-Kutta-Fehlberg methods [32, 33], with appropriate step size selection. The following is an example of a model, and the simulation result is shown in Fig. 7.21.

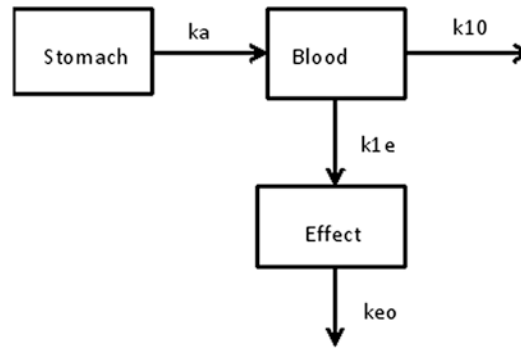

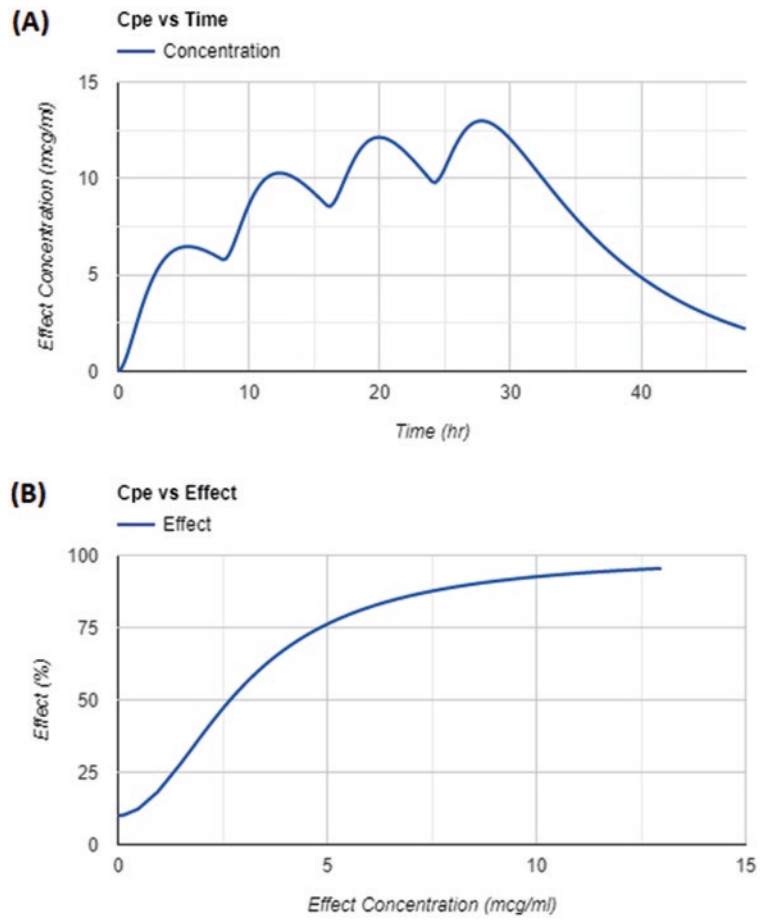

Fig. 7.21 PK/PD simulation plots using the predefined models (1-CBM oral/sigmoid E_{max}) based on the differential equations (**a**) concentrations in an effect compartment (Cp_e) following multiple oral doses and (**b**) the effect vs. effect compartment concentrations. For simulation, parameters used were $K10 = 0.1$ (/hr), $Ka = 1$ (/hr), Ke0 = 0.5 (/hr), $V_d/F = 10$ (L), $EC_{50} = 3$ (mcg/mL), $\gamma = 2$, step size = 0.25, dose = 100 mg q8h for 24 hours, and time frame = 0 to 48 hours

For a one-compartment model and the first-order absorption model shown above, the rate of loss of a drug from the stomach is given by

$$\frac{dXa}{dt} = -ka.Xa \tag{7.32}$$

The rate of absorption by an apparent first-order process and the first-order elimination of a drug from the body are given by

$$\frac{dX}{dt} = ka.Xa - k10.X \tag{7.33}$$

Xa = amount in stomach (initial = dose), X = amount in blood (initial = 0), $X = VC$, ka = apparent first-order absorption rate constant

$k10$ = apparent first-order elimination rate constant

V = apparent volume of distribution of blood compartment

The rate of loss of drug concentration (Ce) from the effect compartment is given by

$$\frac{dCe}{dt} = \frac{ke0.X}{V} - ke0.Ce \tag{7.34}$$

where

$ke0$ = rate constant for drug removal from the effect compartment

30.2 User-Defined Simulation Models

This module provides an interface for the flexibility of writing differential equations and their

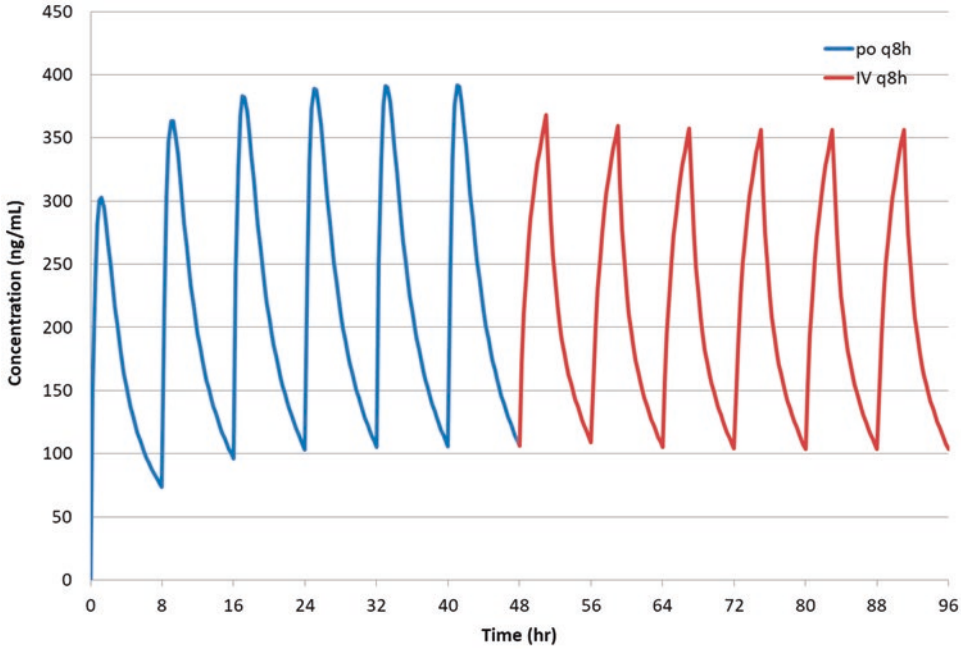

Fig. 7.22 Simulation of plasma concentrations for oral multiple doses followed by a 3-hour IV infusion q8h dosing

integration and visualizing results. The dosing routes, such as IV and extravascular, and combination of these for single and multiple doses can be easily included. The following is an example of multiple-dose oral and IV infusion for a drug with 2-CBM profile (Fig. 7.22).

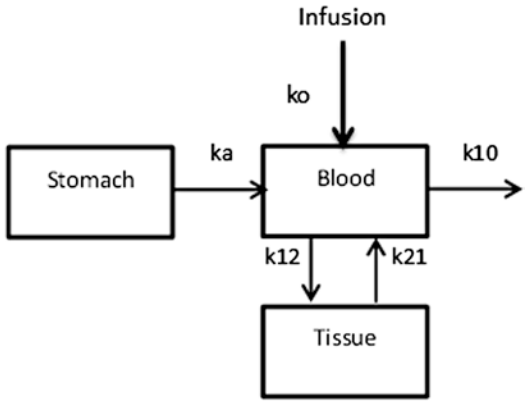

For a two-compartment model and the first-order absorption shown above, the rate of loss from the stomach is given by

$$\frac{dXa}{dt} = -ka \cdot Xa \tag{7.35}$$

The rate of absorption by an apparent first-order process and the rate of change of the drug from the blood (central) compartment by a first-order process are given by

$$\frac{dX}{dt} = ka \cdot Xa - k10 \cdot X - k12 \cdot X + k21 \cdot Xt \tag{7.36}$$

The rate of change of drug levels in the tissue (peripheral) compartment is given by

$$\frac{dXt}{dt} = k12 \cdot X - k21 \cdot Xt \tag{7.37}$$

Xa = amount in stomach
X = amount in blood compartment
Xt = amount in tissue compartment
ka = apparent first-order rate constant
$k10$ = apparent first-order elimination rate constant
$k12$ and $k21$ = apparent first-order inter-compartmental distribution rate constants

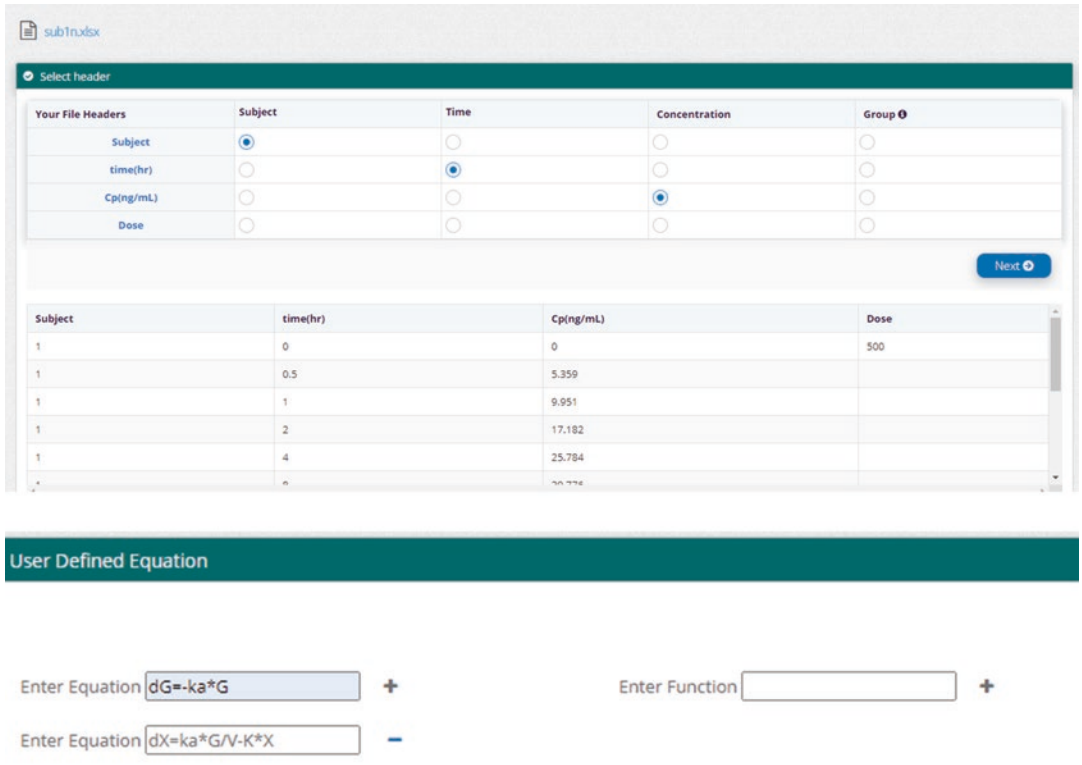

Fig. 7.23 Data input mapping and differential equations

30.3 User-Defined Differential Equation Model Optimization

The experimental data can be fitted to a mathematical model using a set of ordinary differential equations. The following is an example of a data fitted to oral 1-CBM differential equations:

$$dG = -ka.G \tag{7.38}$$

$$dX = ka.\frac{G}{V} - K.X \tag{7.39}$$

where

G = amount of drug in stomach
ka = first-order rate constant for absorption
X = amount of drug in blood
K = first-order elimination rate constant
V = apparent volume of distribution

The data input and differential equations are shown in Fig. 7.23.

The compartment, parameter, constant (for infusion input), and compartment to be optimized are selected as shown in Fig. 7.24.

Initial value of parameters, their upper and lower bound, and dosing information are provided. The optimization is achieved using either a L-BFGS-B [34], Nelder-Mead [14], or Levenberg-Marquardt [35] method using appropriate weight selection. The parameter estimates, their standard errors, and CV% are computed (Table 7.26); in addition, observed and predicted graphs (Fig. 7.25), residual plots (Fig. 7.26), and model diagnostics and iteration results are displayed.

31 Conclusions

Pharmacokinetic modeling software (PKMP) is a web-based commercial program created using the open source codes for Java coding language and *R* libraries. The web-based platform allows

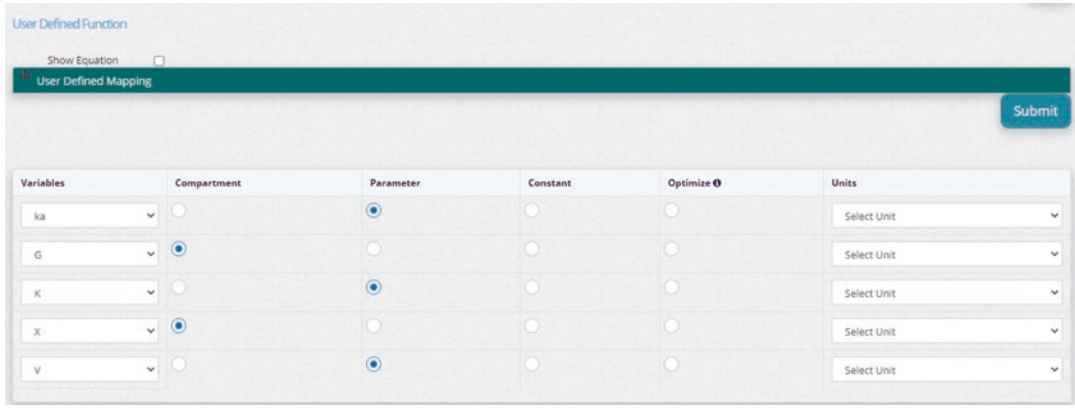

Fig. 7.24 Selection of compartment and parameters for differential equation optimization

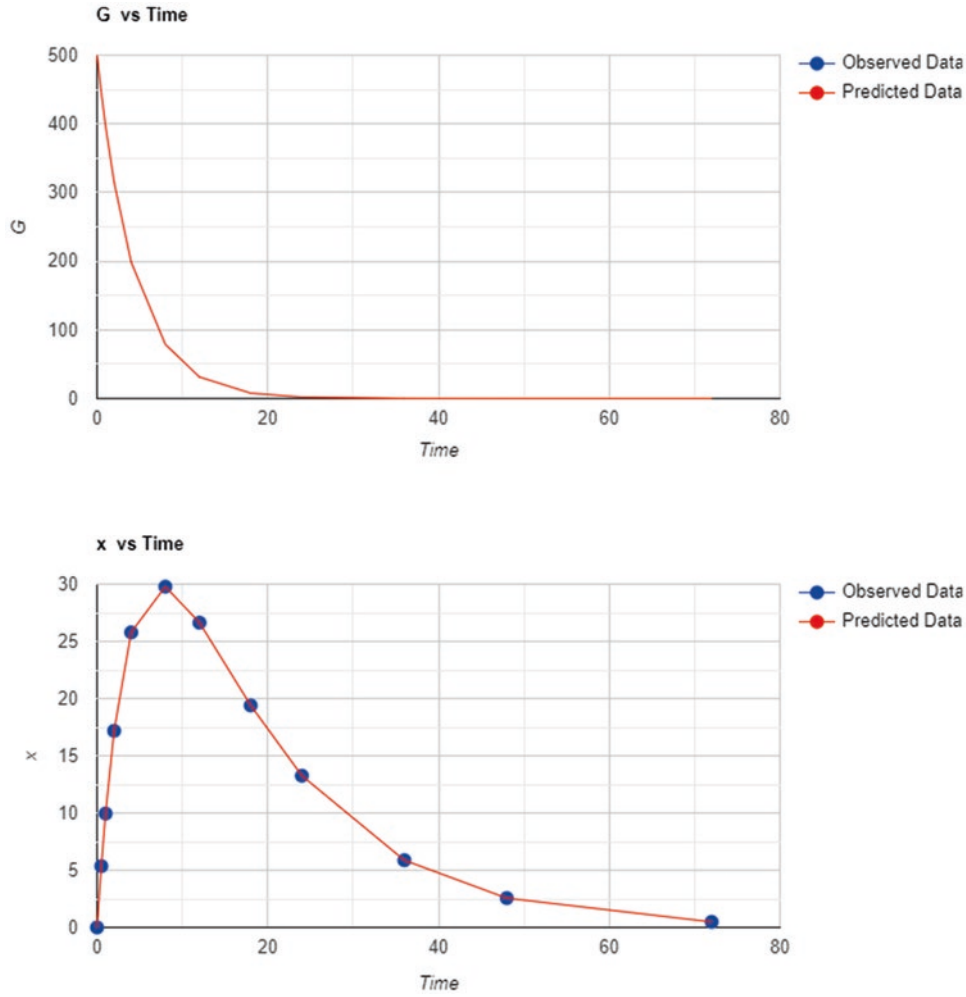

Fig. 7.25 Observed and predicted data for 1-CBM oral data fit using optimization of user-defined differential equations. For *G* compartment data represents amount (mg) and for *X* compartment data is concentration μg/L, and time is in hours

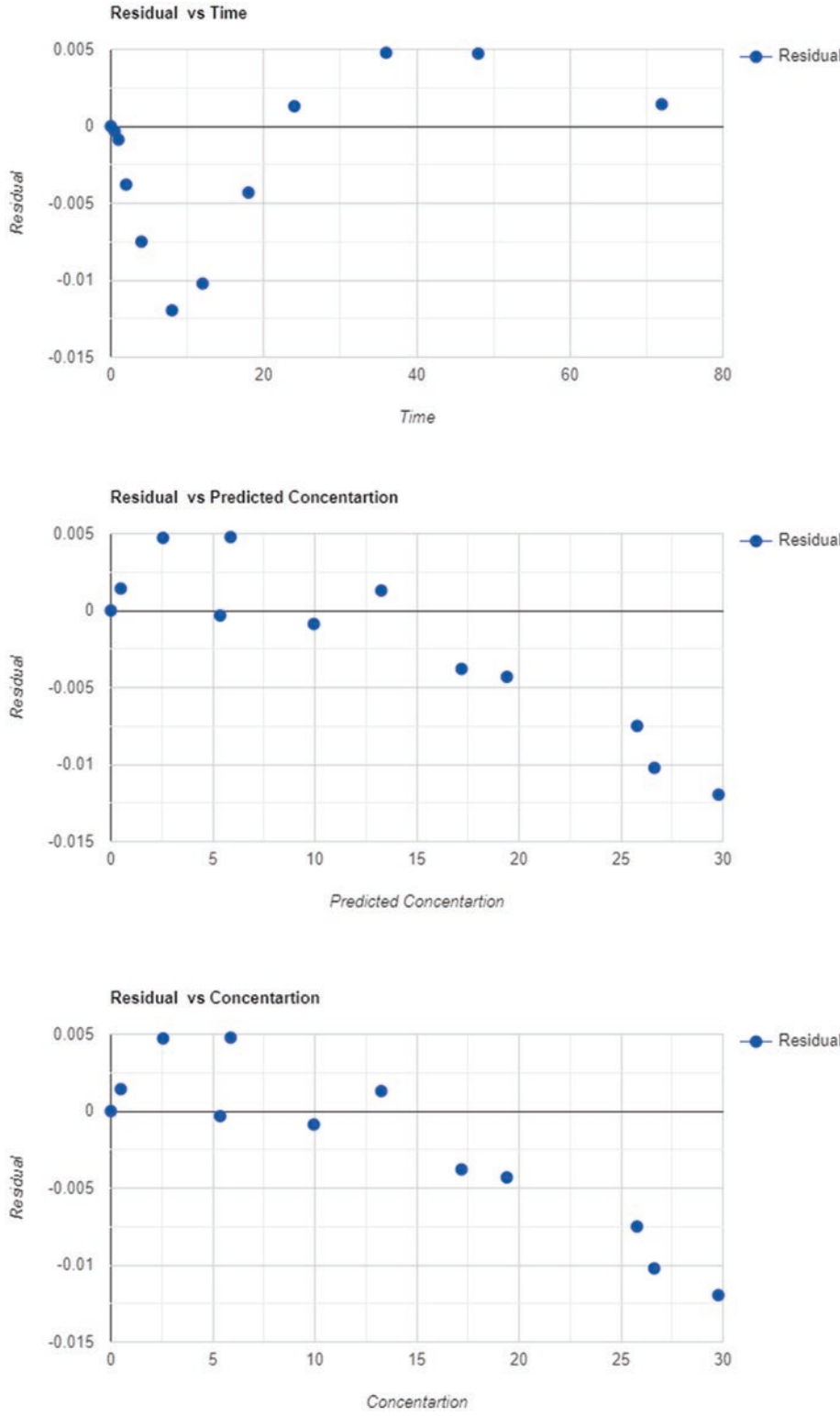

Fig. 7.26 Residual plots for 1-CBM oral data fit using optimization of user-defined differential equations

Table 7.26 1-CBM oral model parameter estimates using user-defined differential equation optimization

Parameter	Estimate	Standard error	CV%
Subject	1		
Ka (/hr)	0.2308	0.0178	7.7123
K (/hr)	0.0694	0.0049	7.0605
V (L)	9.9934	0.5168	5.1714

easy and secure access to the program using any Internet browser, and the program is independent of operating systems, such as MacOS or Windows. The program has been extensively tested for validation and verification of every module for its quality and functionality. Pharmacokinetic, pharmacodynamic, statistical analysis, dissolution, IVIVC, simulation, modeling, and reporting are some of its main functionalities, allowing for a wide range of data analyses to support drug product evaluation and development during different phases of drug development. The program can be accessed at https://aplanalytics.com/.

Acknowledgments The author would like to thank Anupama DS and programmers for their support in developing PKMP as a commercial product. The author is thankful for the critical editorial review by Soham Shah and Dr. Anant Shah.

References

1. Biopharmaceutical Research & Development: The Process Behind New Medicines. http://phrma--docs.phrma.org/sites/default/files/pdf/rd_brochure_022307.pdf.
2. Gibaldi M, Perrier D, editors. Pharmacokinetics. Revised and expanded. 2nd ed. New York: Marcel Dekker Inc; 1982.
3. Welling PG, Tse FLS, editors. Pharmacokinetics regulatory, industrial, academic, perspective. New York: Marcel Dekker, Inc; 1988.
4. Rowland M, Tozer TN. Clinical pharmacokinetics, concepts and application. Philadelphia: Lea and Febiger; 1980.
5. Bulitta JB, Holford NHG. An introductory guide to non-compartmental analysis, In: Wiley encyclopedia of clinical trials. Wiley; 2008. https://doi.org/10.1002/9781118445112.stat06889.
6. Guidance for industry, statistical approaches to establishing bioequivalence: U.S. Department of Health and Human Services Food and Drug Administration, Center for Drug Evaluation and Research (CDER), January 2001.
7. Bailer AJ. Testing for the equality of area under the curves when using destructive measurement techniques. J Pharmacokinet Biopharm. 1988;16:303–9.
8. Mager H, Goller G. Resampling methods in sparse sampling situations in preclinical pharmacokinetic studies. J Pharm Sci. 1988;87:372–8.
9. Boxenbaum H. Interspecies scaling, allometry, physiological time, and the ground plan of pharmacokinetics. J Pharmacokin Bipharm. 1982;10:201–27.
10. Ritschel WA, Vachharajani NN, Johnson RD, Hussain AS. The allometric approach for interspecies scaling of pharmacokinetic parameters. Comp Biochem Physiol. 1992;103C:249–53.
11. Guidance for industry: estimating the maximum safe starting dose in initial clinical trials for therapeutics in adult healthy volunteers. U.S. Department of Health and Human Services Food and Drug Administration, Center for Drug Evaluation and Research (CDER), Pharmacology and Toxicology, July 2005.
12. Penel N, Kramar A. What does a modified-Fibonacci dose-escalation actually correspond to? Med Res Methodol. 2012;12:103:1–5.
13. Gavin HP. The Levenberg-Marquardt algorithm for nonlinear least squares curve-fitting problems, September 18, 2020. http://people.duke.edu/~hpgavin/ce281/lm.pdf.
14. Nelder JA, Mead R. A simplex method for function minimization. Comput J. 1965;7:308–13.
15. Guidance for industry dissolution testing of immediate release solid oral dosage forms. U.S. Department of Health and Human Services Food and Drug Administration Center for Drug Evaluation and Research (CDER), August 1997.
16. Suarez-Sharp S, Abend A, Hoffelder T, Leblond D, et al. In vitro dissolution profiles similarity assessment in support of drug product quality: what, how, when—workshop summary report. AAPS J. 2020;22:74. https://doi.org/10.1208/s12248-020-00458-9.
17. Dash S, Murthy PN, Nath L, Chowdhury P. Kinetic modeling on drug release from controlled drug delivery systems. Acta Pol Pharm Drug Res. 2010;67:217–23.
18. Kalam MA, Humayun M, Parvez N, Yadav S, Garg A, Amin S, Sultana Y, Ali A. Release kinetics of modified pharmaceutical dosage forms: a review. Cont J Pharm Sci. 2007;1:30–5.
19. Moore JW, Flanner HH. Mathematical comparison of dissolution profiles. Pharm Technol. 1996;20:64–74.
20. Tanigawara Y, Yamaoka K, Nakagawa T, Uno T. New method for the evaluation of in vitro dissolution time and disintegration time. Chem Pharm Bull. 1982;30:1088–90.
21. Tsong Y, Hammerstrom T, Sathe P, Shah VP. Statistical assessment of mean differences between two dissolution data sets. Drug Inf J. 1996;30:1105–12.
22. FDA. Guidance for industry: extended release oral dosage forms: development, evaluation, and applica-

tion of in vitro/in vivo correlations, September 1997. http://www.fda.gov/cder/guidance/index.htm.
23. Gillespie WR. Convolution based approaches for in vivo in vitro correlation modeling, in vitro in vivo correlations. Adv Exp Med Biol. 1997;423:53–65.
24. Gillespie WR. Modeling strategies for in vivo in vitro correlations. In: Amidon G, Robinson JR, and Williams RL, editors. Scientific foundation for regulating drug product quality. Alexandria: AAPS Press; 1997. p. 275–92.
25. Qureshi SA. In Vitro-In Vivo Correlation (IVIVC) and determining drug concentrations in blood from dissolution testing – a simple and practical approach. Open Drug Delivery J. 2010;4:38–47.
26. Langenbucher F. Handling of computational in vitro/in vivo correlation problems by Microsoft Excel: III. Convolution and deconvolution. Eur J Pharm Biopharm. 2003;56:429–37.
27. Langenbucher F. Numerical convolution deconvolution as a tool for correlating in vitro and in vivo drug availability. Pharm Ind. 1982;44:1166–71.
28. Langenbucher F. Improved understanding of convolution algorithms correlating body response with drug input. Pharm Ind. 1982;44:1275–8.
29. Loo LCK, Riegelman S. A new method for calculating intrinsic absorption rates of drugs. J Pharm Sci. 1968;57:918–28.
30. Wagner JG, Metzler C. Estimation of rate constants for absorption and elimination from blood concentration data. J Pharm Sci. 1967;56:658–9.
31. Diletti E, Hauschke D, Steinijans VW. Sample size determination for bioequivalence assessment by means of confidence intervals. Int J Clin Pharmacol Therapy Toxicol. 1991;29(1):1–8.
32. Cash JR, Karp AH. A variable order Runge-Kutta method for initial value problems with rapidly varying right-hand sides. ACM Trans Math Softw. 1990;16(3):201–22.
33. Michael Thomas Flanagan's Java Scientific Library RungeKutta Class: Numerical Solution of Differential Equations. https://www.ee.ucl.ac.uk/~mflanaga/java/RungeKutta.html.
34. Byrd RH, Lut P, Nocedalt J, Zhu C. A limited memory algorithm for bound constrained optimization. SIAM J Sci Comput. 1995:16(5):1190–208.
35. Gavin HP. The Levenberg-Marquardt algorithm for nonlinear least squares curve-fitting problems. https://people.duke.edu/~hpgavin/ce281/lm.pdf.